Copyright Warning & Restrictions

The copyright law of the United States (Title 17, United States Code) governs the making of photocopies or other reproductions of copyrighted material.

Under certain conditions specified in the law, libraries and archives are authorized to furnish a photocopy or other reproduction. One of these specified conditions is that the photocopy or reproduction is not to be "used for any purpose other than private study, scholarship, or research." If a, user makes a request for, or later uses, a photocopy or reproduction for purposes in excess of "fair use" that user may be liable for copyright infringement,

This institution reserves the right to refuse to accept a copying order if, in its judgment, fulfillment of the order would involve violation of copyright law.

Please Note: The author retains the copyright while the New Jersey Institute of Technology reserves the right to distribute this thesis or dissertation

Printing note: If you do not wish to print this page, then select "Pages from: first page # to: last page #" on the print dialog screen

ABSTRACT

LOW PRESSURE CHEMICAL VAPOR DEPOSITION OF COPPER FILMS FROM CU(I)(HFAC)(TMVS)

by
Wei-Shang King

Recently, copper has been found as a possible substitute for Al alloys because of its low resistivity (1.67 $\mu\Omega \cdot$ cm) and potentially improved resistance to electromigration. Conventional physical vapor deposition (PVD) method do not provide the conformal deposition profile for the high density integrated circuit, therefore, chemical vapor deposition (CVD) has become the most promising method for the resulting conformal profile.

In this work, a cold wall, single wafer, CVD tungsten reactor was used for the deposition of copper with Cu(I)(hfac)(tmvs). Film growth rates were between 100 to 800 Å/min depending on processing conditions, and an Arrhenius type activation energy of 16.1 kcal/mole was obtained in the temperature region of 150-180 °C. No significant amount of contamination is detected in the copper films, and the resistivity of the films was routinely near 2.2 $\mu\Omega \cdot$ cm when the film was 5000 Å or more. The surface roughness of the films increased with increasing film thickness, and the crystal orientation was found as a function of growth rate. These obtained results demonstrated the feasibility of using Cu(I)(hfac)(tmvs) in the synthesis of high purity copper films using liquid injection by LPCVD.

LOW PRESSURE CHEMICAL VAPOR DEPOSITION OF COPPER FILMS FROM CU(I)(HFAC)(TMVS)

by
Wei-Shang King

A Thesis
Submitted to the Faculty of
New Jersey Institute of Technology
in Partial Fulfillment of the Requirements for the Degree of
Master of Science in Engineering Science

Interdicipplinary Program in Materials Science and Engineering

January 1995

APPROVAL PAGE

LOW PRESSURE CHEMICAL VAPOR DEPOSITION OF COPPER FILMS FROM CU(I)(HFAC)(TMVS)

Wei-Shang King

Dr. Roland A. Levy, Thesis Advisor — Date
Professor of Physics,
Director of Materials Science and Engineering program, NJIT

Dr. James M. Grow, Thesis Advisor — Date
Professor of Chemical Engineering, Chemistry, and
Environmental Science, NJIT

Dr. David Kristol — Date
Professor of Chemistry,
Director of Biomedical Engineering Program, NJIT

BIOGRAPHICAL SKETCH

Author: Wei-Shang King

Degree: Master of Science in Engineering Science

Date: January 1995

Undergraduate and Graduate Education:

- Master of Science in Engineering Science,
  New Jersey Institute of Technology,
  Newark, New Jersey, January 1995

- Bachelor of Science in Chemical Engineering,
  Chinese Culture University
  Taipei, Republic of China, June 1989

Major: Materials Science and Engineering

This thesis is dedicated to
my parents, Yuo-Jung King and Hsuen-Lian King Lee

ACKNOWLEDGMENT

The author wishes to express his sincere gratitude to his advisors, Professor Roland A. Levy and James M. Grow, for their guidance, friendship, moral and financial support throughout this thesis work, without which it would not have been completed.

Special thanks to Professor David Kristol for serving as member of the committee.

The author appreciates the timely help and suggestions from the CVD Lab. members, including: Roumiana Petrova, Venkat Paturi, Mahalingam Bhaskaran, Shingo Uto, Yan Gao, Xin Lin, Hong Wang, Abhijit Datta, Jan Opyrchal and especially to Vitaly Sigal for his invaluable technical assistance, co-worker David Perese who provided assistance on all aspects of this project, Chenna Ravindranadh who provided the X-ray diffraction data, and Wei-Ching Liang who taught the author the techniques of Rutherford Backscattering Spectroscopy (RBS) at Bell Labs, Murry Hill, N.J. Finally, the author wishes to acknowledge Jose Albella who began the work that provided the necessary foundation for this paper.

TABLE OF CONTENTS

TABLE OF CONTENTS
(Continued)

TABLE OF CONTENTS
(Continued)

LIST OF TABLES

LIST OF FIGURES

LIST OF FIGURES
(Continued)

CHAPTER 1

INTRODUCTION

1.1 Cu - The Most Promising Metal of Interconnect in The Future

Aluminum has been the main interconnect material for a long time in integrated circuits (IC) because it fulfills most of the requirements for silicon integrated circuits. However, it is being projected that the performance of the next generation ICs with higher device densities, faster operating frequencies, and large sizes may be limited by the interconnects [1][2]. Therefore, new materials must be investigated for contacts and interconnects as an alternative to aluminum metallization, especially performance and reliability concerns for these approaches have led to consideration of low resistivity material, such as copper. Theoretically, copper exhibits pronounced advantages (such as low resistivity, high resistance to electromigration and stress, high melting point) over aluminum as a high density interconnect material [3]. In this chapter, a brief summary of the importance of interconnects for ULSI is present. The requirements of general interconnect metallization, aluminum and copper metallization are discussed. Finally, the general concept of CVD (Chemical Vapor Deposition) techniques are introduced.

1.1.1 The Advanced Interconnection for ULSI (VLSI)

In the microelectronics industry, integrated circuit (IC) device performance is continually increasing while the critical feature sizes are rapidly decreasing [4]. The

demand for manufacturing integrated circuit (IC) devices with high circuit speed, high packing density and low power dissipation requires the downward scaling of feature size in ultralarge-scale integration (ULSI) structures since the area density constraints often require that circuit designs utilize multilevel structures with vertical interconnects [1]. When chip size becomes smaller, the propagation time delay in a device is reduced. However, the importance of on-chip interconnect RC (resistance capacitance) delay to chip performance, reliability, and processing cost is increasing dramatically.

When interconnect feature size decreases and clock frequencies increase, RC time delays become the major limitation in achieving high circuit speeds. The miniaturization of interconnect feature size also severely penalizes the overall performance of the interconnect, such as increasing interconnect resistance and interconnect current densities, which lead to reliability concerns due to electromigration [1][5]. Lower resistance metal and lower dielectric materials are being considered to replace current Al and SiO_2 interconnect materials [6].

Interconnect feature sizes can be miniaturized by reducing the wiring pitch and adding more metallization levels. Reducing interconnect pitch increases wiring resistance and the wire's parasitic capacitance, causing more crosstalk noise. Scaling down interconnect width without shrinking interconnect thickness can suppress the increase in interconnect resistance [1][7]. This can be achieved by increasing the aspect ratio (ratio of height to width) of the interconnect wiring, because the interconnect resistance in a metal line increases as its cross-sectional area decreases (resistance=resistivity×(length/cross-sectional area)) [8]. Therefore, a good step coverage of metallization would become

necessary. For instance, poor step coverage of a metal may cause higher interconnect resistance and electromigration failure.

The requirements of circuit density and performance are increasing while circuit dimensions decrease [4]. As a result of this trend, the new material for deep submicron ULSIs must have low resistivity and higher resistance to electro- migration and stress migration than does aluminum alloy so copper is an attractive material for future generations of ICs.

1.1.2 Requirements for Interconnect Structure Metallization

In selecting a material for metallization, many factors should be considered, but it may be impossible to find a material with all the benefits without sacrificing some important properties. The following properties of metallization for integrated circuits are very important:

(1) low electrical resistivity.

(2) good resistance to electromigration.

(3) easy deposition.

(4) good resistance to stress-induced voiding.

(5) good resistance to oxidation.

(6) conformal deposition.

(7) good adhesion with dielectrics.

(8) easy dry-etching.

(9) high mechanical strength.

(10) good thermal stability

(11) the existence of a high volatility, non toxic precursor.

(12) low cost.

(13) no contamination on device.

1.1.3 Aluminum Metallization and Its Limitation

Aluminum or an aluminum alloys are now generally used as the interconnecter material in LSI circuits because the physical and chemical properties of aluminum are compatible with current LSI processing; aluminum forms a thin protective oxide film that withstands various thermal processes; it has relatively low electrical resistivity, superb adhesion to the underlying dielectric layers on which halide compounds with a relatively high vapor pressure are suitable for reactive ion etching (RIE), and it is an inexpensive material. The Al-based metallization has not changed extensively except for alloying with Cu to improve the reliability [9], with a small amount of silicon to prevent Al spiking [10].

Currently, Al and its alloys are the major interconnect materials. SiO_2 is commonly used as a dielectric material due to its low dielectric constant of 3.9 [1]. However, the minimum feature size in an integrated circuit (IC) has been decreasing in order to increase the speed and device density and decrease the chip size. The trend is detrimental to the interconnections, because the cross-sectional area of interconnect decreases as the device dimension is scaled down and the length of the interconnect increases as the chip size increases. Aluminum-based metallization does face several serious problems as stated below concerning its performance and reliability.

(1) high line resistance, which will limit the operation speed.

(2) poor electromigration resistance, which will restrict the current carrying capability.

(3) low melting point which is responsible for its high reactivity with silicon [12].

(4) stress-induced voiding , which shortens its lifetime [11].

(5) hillock formation which will cause inter-level short circuits and complicate multilevel metallization.[11][13].

To improve such performance limitations, aluminum alloys are used, but the alloys show a relatively high resistivity, 3 to 4 $\mu\Omega \cdot cm$ at 0.5 to 1.5 μm. Thus, other metallization materials are being studied seriously as candidates for replacing aluminum[13].

1.1.4 Properties Comparison with Other Metals

In searching for a new metal to substitute for aluminum, the most important factor is the resistivity. In Table 1 the electrical properties (bulk resistivity, temperature coefficient of resistivity), physical properties (melting point, atomic weight) and mechanical properties (Young's modulus, ultimate tensile strength, hardness) of elements aluminum (Al), copper (Cu), gold (Au), silver (Ag) and tungsten (W) are given. The resistivity is not the only factor concerned, thermal stability , resistance to electromigration, stress migration, oxidation, and corrosion are also important. These elements are chosen to be candidates for their special properties such as lower resistivities, high melting point, atomic weight, high mechanical strength, etc.

Theoretically, a metal with high atomic weight should have high resistivity to electomigration, a high melting point and thermal stablility. From the Table 1 it can be seen that Cu, Ag and Au have lower electrical resistivities than aluminum and are expected to have electromigration resistance superior to that of aluminum. Also important is that they are mechanically stronger than aluminum. Even though the electrical resistivity of Ag is the lowest one, the agglomeration behavior and severe migration problem of the thin silver film make it difficult for it to be compatible with integrated circuit processes. From the commercial consideration Au is not worth the huge amount of investment to become the substitute because of its cost.

Property \ Metal	Al	Cu	Au	Ag	W
Electrical Properties of Metal					
Bulk Resistivity at 20°C($\mu\Omega \cdot cm$)	2.67	1.69	2.2	1.63	5.4
Temperature Coefficient of Resistivity at 0 - 100°C($10^{-3}/K$)	4.5	4.3	4.0	4.1	4.8
Physical Properties of Metal					
Melting Point (°C)	660.1	1083.4	1063	960.8	3400
Atomic Weight ($^{12}C=12$)	26.98	63.54	196.9	107.8	183.8
Mechanical Properties of Metal					
Young's Modulus (Gpa)	70.6	129.8	78.5	82.7	411.0
Hardness (HV)	15	51	20-30	25	360
Ultimate Tensile Strength (Mpa)	55	216	130	172	550-620

Table 1 Electrical, Physical and Mechanical Properties of Metals.

Cu is the most promising candidate metal for an aluminum replacement. Copper is so attractive because of its some special properties compared to other metals. In addition, it can conformal step coverage, and complete trench filling in the fabrication of multilevel metallization schemes. Many obstacles to the use of copper still exist in VLSI and ULSI processing. For instance, copper dry etching is difficult because the vapor pressure of most copper halides is low at room temperature. The relatively low interfacial reaction temperatures between copper and most contact materials cause a serious thermal stability problem in copper-based metallization.

1.1.5 Copper Metallization

In order to compare copper with aluminum as shown in Table 2 [33] shows some important characteristics for integrated circuit application. There are several important factors which can prove that the Cu is worth investigating for a replacement of aluminum alloy for chip interconnections, these factors [10] are:

(1) the low resistivity of Copper (1.7 $\mu\Omega$ cm at 22 °C) is its prime advantage, the resistivity of pure aluminum (2.7 $\mu\Omega$ cm) is actually not obtained in current interconnections, since Aluminum is alloyed with copper. Copper has about 30%-50% lower resistivity than Aluminum, that can increase the operation speed in a device, especially with deep sub-micron feature size [1][14][15].

(2) the Copper interconnect lines have a high activation energy against electromigration, up to twice as large as that of aluminum [1][14][28].

(3) to achieve the same resistance of interconnect lines, the thickness of a copper line can be thinner than that of Aluminum, the thinner interconnect lines can make chemical vapor deposition (CVD) trench filling and planarization easier [1].

(4) a combination of proper barrier metal and new patterning technology (such as chemical-mechanical polishing) seems to circumvent most of the potential problem [16].

(5) Copper can be deposited by plating (such as electroless and electrolytic), sputtering (physical vapor deposition, PVD), laser-induced reflow , and CVD.

Metal / Property	Cu	Al
Electrical Resistivity	excellent	good
Electromigration Resistance	good or excellent	poor
Stress-Induced Voiding Resistance	good or excellent	poor
Mechanical Strength	strong	weak
Oxidation Resistance	poor	good
Corrosion Resistance	poor	poor
Ease of Deposition	easy	easy
Ease of Dry-Etching	difficult	easy
Conformal Deposition (CVD)	excellent	good
Conformal Deposition (PVD)	poor	poor
Smoothness of Surface	good or excellent	poor
Adhesion with Dielectrics	poor	good
Contamination on Devices	severe	none

Table 2 Properties Comparison with Cu and Al.

Significant improvement in reliability and performance over that achievable with aluminum alloys must be demonstrated first. Toward this purpose, processes need to be developed that deposit conformal copper films of high purity with acceptable throughput, and integration schemes need to be developed which produce interconnects and multilevel metal structures with reliability significantly better than that of aluminum [5].

1.2 Fundamentals of Chemical Vapor Deposition

1.2.1 Introduction

Chemical vapor deposition (CVD). CVD is a process whereby a thin solid film is synthesized from the gaseous phase by a chemical reaction. It is this reactive process which distinguishes CVD from physical deposition processes, such as evaporation, sputtering and sublimation [17].

Chemical vapor deposition (CVD) is a very versatile process used in the production of coatings, powders, fibers and monolithic components. With CVD, it is possible to produce almost any metal and non-metallic element, including carbon or silicon, as well as compounds such as carbides, nitrides, oxides, intermetallics and many others. This technology is now an essential factor in manufacture of semiconductors and other electronic components, in the coating of tools, bearings and other wear resistant parts, and in many optical, opto-electronic and corrosion applications [18].

1.2.2 Principles and Mechanisms of CVD

Chemical Vapor Deposition is a synthesis process in which the chemical constituents react

in the vapor phase near or on a substrate to form a solid deposit. It combine several scientific and engineering disciplines including thermodynamics, plasma physics, kinetics, fluid dynamics and, of course chemistry[18]. The chemical reactions used in CVD are numerous and include thermal decomposition (pyrolysis), reduction, hydrolysis, disproportionation, oxidation, which can be used either singly or in combination.

The individual process steps are displayed schematically in Figure 1.1 and may be summarized in terms of the following deposition sequence:

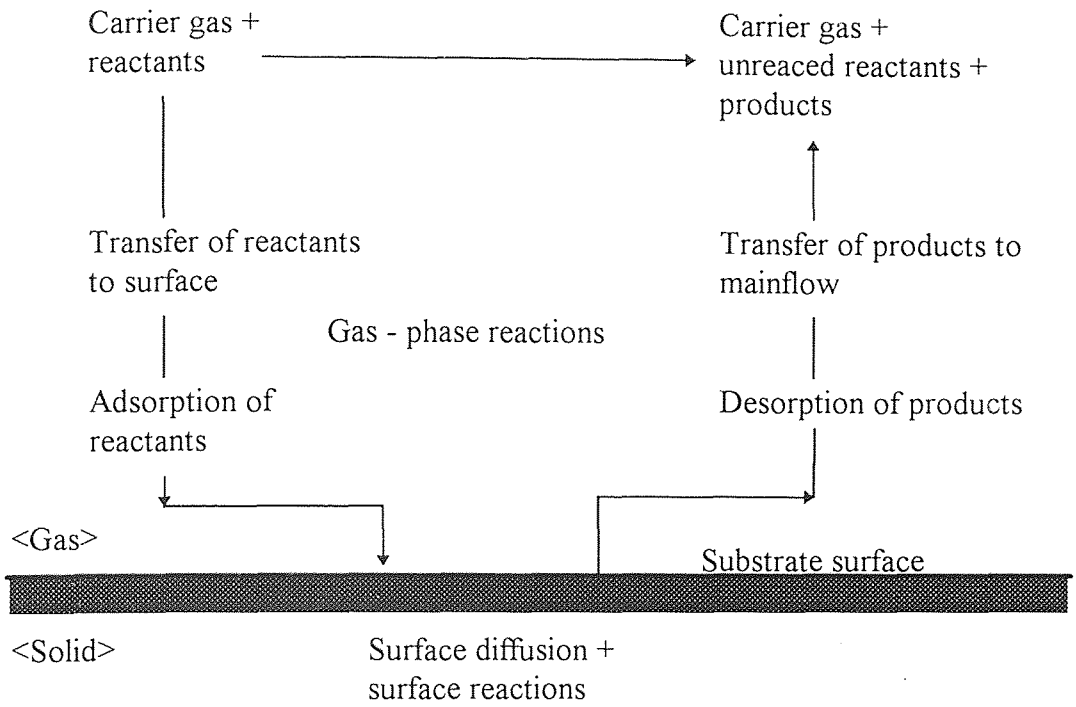

Figure 1.1 Processes contributing to CVD growth.

(1) mass transport in the gas flow region from the reactor inlet to the deposition zone;

(2) gas phase reactions leading to the formation of film precursors and byproducts;

(3) mass transport of film precursors on the growth surface;

(4) adsorption of film precursors on the growth surface;

(5) surface diffusion of film precursors to growth sites;

(6) incorporation of film constituents into the growing film;

(7) desorption of byproducts of the surface reactions; and

(8) mass transport of byproducts in the gas flow region away from the deposition zone towards the reactor exit.

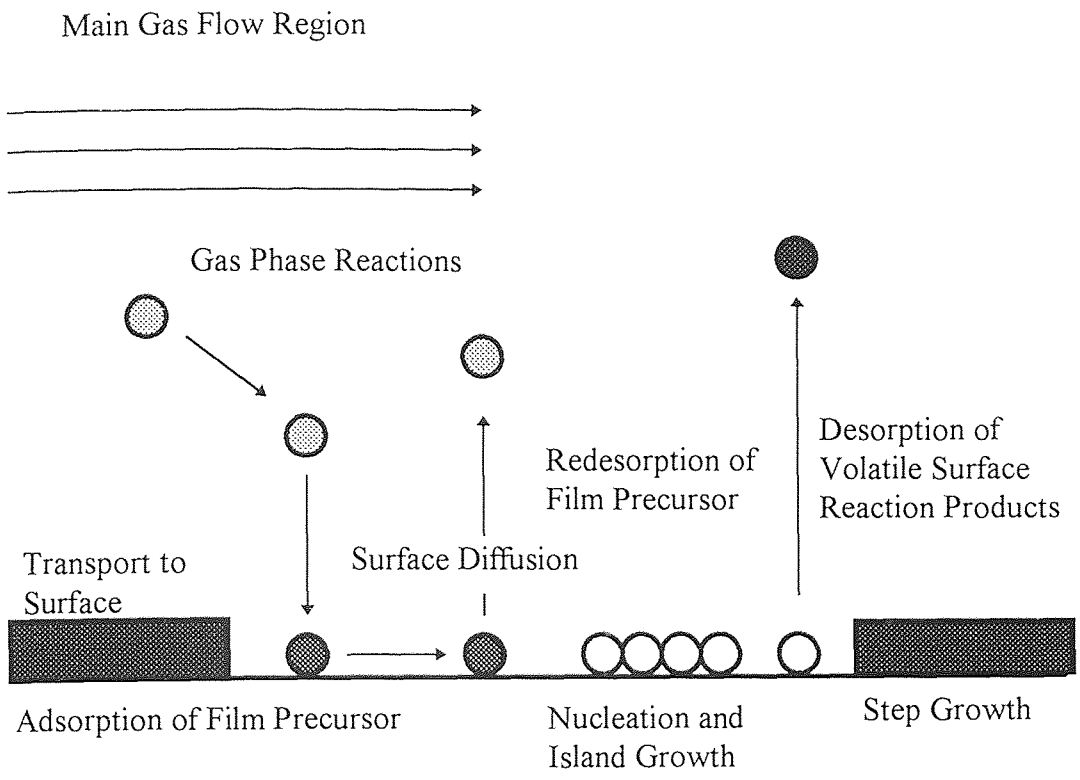

Figure 1.2 Scheme to show the transport and reaction processes underlying CVD.

Each step in Figure 1.2 which schematically showed the transport and reaction processes underlying CVD must be controlled in order for CVD to deposit thin films of uniform composition and film thickness with desired materials properties[17]. The energy required to drive the reactions can be supplied by several methods including heat, photons, and ions, with thermal energy being the most commonly used [18].

Basically, There are two kinds of chemical reactions leading to the formation of a solid material [22], one is heterogeneous reaction that occurs on (or very close to) the wafer surface, the other one is homogeneous reaction that take place in the gas phase. Homogeneous reactions whose chemistry are generally undesirable since they form gas phase clusters which lead to poor quality films (rough, poorly adherent deposits). However, heterogeneous reactions are more desirable because they occur only on the substrate surface (good selectivity) and can produce good quality films.

1.2.2.1 Rate Limiting Steps

The rate limiting step of a CVD reaction is that step which controls the growth rate of the deposition? The rate limiting step can be

(a) the surface reaction kinetics,

(b) the mass transport,

(c) gas-phase kinetics.

In the case of control by surface reaction kinetics, the rate is dependent on the amount of reactant gases available on the surface [18].

As shown in Figure 1.3, a CVD system with low temperature and low pressure means that the reaction occurs slowly on the surface, the boundary layer is thin, the diffusion coefficients are large, and the reactants reach the deposition surface with ease. Adversely, the process is limited by mass transport phenomena, as shown in Figure 1.4, a CVD system with high temperature and high pressure the controlling factors are the diffusion rate of the reactant through the boundary layer and the diffusion out through this layer of the gaseous by-products [18].

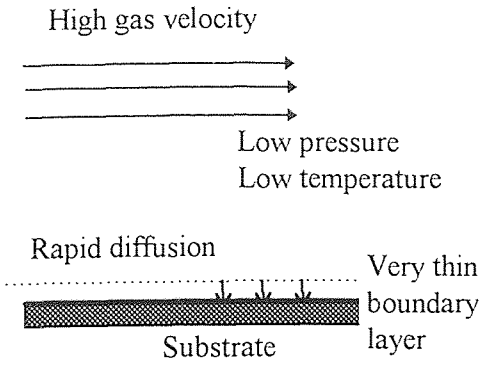

Figure 1.3 Surface reaction kinetics control

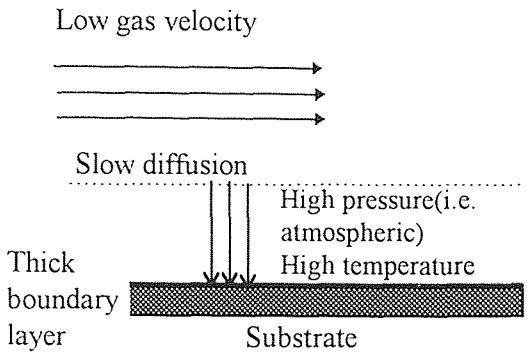

Figure 1.4 Diffusion control

1.2.2.2 Temperature Dependence

The temperature dependence of deposition rate in a heterogeneous mechanism generally follows the empirical Arrhenius behavior of the type,

$$Deposition\ Rate \propto k_0 \cdot e^{-Ea/RT}$$

where k_0 is pre-exponential factor, R is the gas constant, T is the absolute temperature, and Ea is the activation energy [22,23]. As a result, since normally the surface reaction kinetics (or near surface reaction kinetics) are the rate limiting step at lower temperature and diffusion is the rate limiting step at higher temperature, it is possible to switch from one rate limiting step to the other by changing the temperature as shown in Figure 1.5 in the Arrhenius plot (the deposition rate vs the reciprocal temperature) [18].

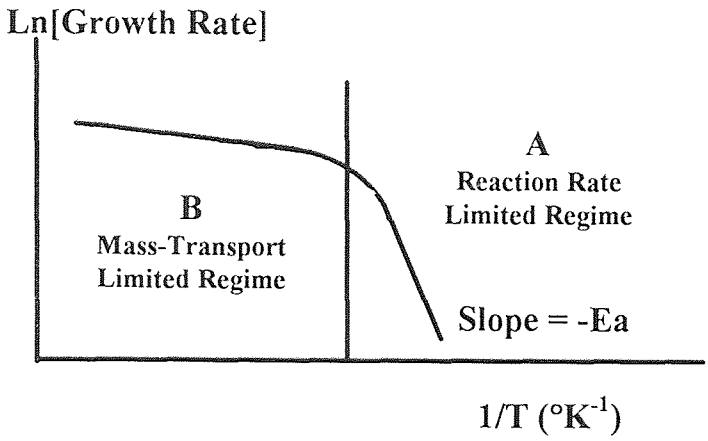

Figure 1.5 Variation of deposition rate as a function of reciprocal temperature for typical CVD process.

In the A sector, the deposition is controlled by surface reaction kinetics as the rate limiting step. In the B sector, the deposition is controlled by the mass transport process and the growth rate is related linearly to the partial pressure of the reactant in the carrier gas. The presence of a maximum in the curves in Area B could indicate the onset of gas-phase precipitation, where the substrate has become starved and the deposition rate decreased [18].

In actual processes, the temperature at which the critical point moves from one growth regime to the other depends on activation energy and gas flow conditions [17].

1.2.3 CVD System

CVD reactors must be designed and operated in such a manner that film thickness, crystal structure, surface morphology, and interface composition changes can be accurately controlled. Basically, CVD system should contain the following components:

(a) Gas sources,

(b) Gas feed lines,

(c) Mass-flow controllers (for metering the gases into the system),

(d) A reaction chamber,

(e) Means of heating the substrates onto which the film is to be deposited,

(f) Temperature sensors,

(g) Vacuum pumps for achieving reduced pressures and exhausting reactants.

1.2.4 Categories of CVD

1.2.4.1 Introduction

Cu-based interconnects will represent the future trend in the deep submicron regime. Table 3 [1] lists the properties of Cu films obtained by different deposition methods. Plating-based deposition can provide high deposition rates and low tool cost, but the wet

	CVD	PVD	Laser reflow	Electroless	Electrolytic
Resistivity ($\mu\Omega\times$cm)	≥2	1.75-2	2.6	~2	~2
Impurities	C, O	Ar	—	seed layer	—
Deposition rate(nm/min)	~100	≥100	—	≤100	~200
Process temp.(°C)	~250	RT	melt	50-60	RT
Step coverage	good	fair	—	good	good
Via-filling capability	good	poor	good	fair-poor	fair-poor
Environmental impact (waste)	good	good	good	poor	poor

Table 3 Properties of copper from different deposition methods.

chemical disposal gives rise to serious environmental concerns and may limit the use of copper in IC manufacturing. Cu PVD is a conventional technology with high deposition rate, but poor via-filling and step coverage are the concerns. The laser reflow technique exhibits less compatibility with current VLSI processing. Based on these comparisons, Cu CVD is the most attractive approach for copper-based multilevel interconnects in ULSI chips [1].

1.2.4.2 Laser CVD (LCVD)

Laser CVD occurs as a result of the thermal energy from the laser coming in contact with and heating an absorbing substrate. The wavelength of the laser is such that little or no energy is absorbed by the gas molecules. The substrate is locally heated in a manner

analogous to the local heating in a cold-wall reactor and deposition is restricted to the heated area as shown in Figure 1.6 [18] which illustrates the deposition of a thin stripe .

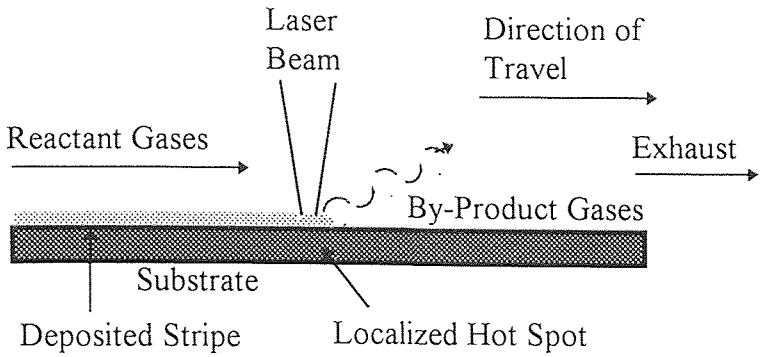

Figure 1.6 Schematic diagram of laser CVD growth mechanism.

The major use so far of laser CVD has been in the direct writing of thin films in semiconductor applications, using holographic methods to deposit complete patterns in a single step with width as small as 0.5 micron.

1.2.4.3 Low Pressure CVD (LPCVD)

LPCVD is categorized by its low operating pressure (0.2-2.0 Torr). Most LPCVD process are conducted by resistance heating to attain isothermal conditions so that the substrate and the reactor walls are of similar temperature. The LPCVD boundary layer is thicker by a factor of 3-10 than that of APCVD [22]. Thus, by operating at low pressure (0.20-2.0 Torr) and higher temperature (550-850 °C), LPCVD processes enhance mass transfer greatly, making it possible to synthesize films in a highly economical close spaced

positioning of the substrate wafers [20]. The surface reaction rate is very sensitive to temperature but precise control of temperature is relatively easy to achieve.

LPCVD techniques started in 1973 with the work by Tanikawa, et al. [23], who realized from reduced pressure deposition principles that closely packed vertical positioning of the substrate wafers is possible, yielding greatly increased throughput in film deposition for a variety of films without loss of uniformity. In 1975 a patent was issued to Chruma and Hilton [24] for LPCVD of polycrystalline silicon from SiH_4. Since then efforts have been made in the past two decades which have led to the remarkably rapid acceptance of this economical technique for production applications to develop LPCVD techniques.

Basic parameters which govern the deposition rate and uniformity of films in LPCVD processes are: 1) temperature profile in the reactor; 2) the pressure level in the reactor; 3) the reactant gas flow rates; and 4) the reactant gas ratios. To obtain a flat thickness profile across each substrate wafer, and from wafer to wafer throughout the reaction chamber, a judicious adjustment of these parameters is required. A precise control of these parameters can result in uniform films.

1.2.5 The Advantages and Disadvantages of LPCVD

1.2.5.1 The Advantages of LPCVD

(1) Low pressure operation decreases gas phase reactions, making LPCVD films less subject to particulate contamination and thus have fewer defects and pin holes.

(2) A great variety of films including polysilicon, silicon nitride, silicon dioxide, boron nitride, and tungsten can be synthesized by LPCVD.

(3) Stoichiometric compositions of the films can be achieved by optimizing LPCVD process parameters.

(4) Uniform film thickness and conformal step coverage can be achieved by LPCVD.

(5) The cost of LPCVD is economical because of its high throughput and low maintenance cost.

1.2.5.2 The Disadvantages of LPCVD

(1) The use of toxic, explosive or corrosive gaseous reactants.

(2) The use of comparatively high temperature.

CHAPTER 2

THE METALLIZATION PROCESS OF COPPER THIN FILM

2.1 Introduction

The chemical vapor deposition of copper is carried out when the volatile liquid precursor is transported directly into the reactor by nitrogen. The deposition on the heated substrate occurs either through decomposition in the gas phase leading to copper, or decomposition of a species adsorbed on the substrate surface into copper and volatile gaseous by-products which desorb and are pumped out. The catalytic function of the substrate surface provides the possibility of selective growth, good coverage, and conformal blanket deposition depending on the Cu CVD reaction conditions.

2.2 Experimental Procedure

2.2.1 Equipment Set Up

The deposition reaction was carried out in a SPECTRUM model 211, cold wall, single wafer CVD tungsten reactor system fully automated computer control as shown in Figure 2.1. In this system 10 cm diameter silicon wafers which are loaded through a load-lock by a casette-to-casette transport facility, are heated on the backside by means of a set of quartz lamps, that are separated from the reactor by a quartz window. When the wafers were transported into the reactor, they will be fixed up against the window by four small pins, leaving the front side exposed to the reactant gases.

The Cu precursor, Cu(I)(hfac) (tmvs), was provided by Schumacher Inc., in an stainless steel container, which was directly attached to the reactor trough a capillary tube of 5 m length and 0.001 mm internal diameter. The capillary tube passed throughout a blind port of the reactor ending just 2 cm below the sample surface. The mass flow through the capillary tube was calibrated against the nitrogen gas pressure in the bottle, thus allowing an easy control of the liquid into the reactor. A sketch of the reactor and the liquid injection system is given in Figure 2.1.

Temperature, pressure and flow rate are the most important three factors for reaction condition control. Temperature can be monitored by means of a thermocouple attached to the back of the wafer and a throttle valve can keep adjusting the efficiency of pumping in order to keep reactor total pressure at the set point. The flow rate of the liquid precursor, which was pushed through the reactor by means of nitrogen stream, can not be read directly. The calibration line as shown in Figure 2.2 was the basis for the Cu(I)(hfac)(tmvs) precursor flow rate determination.

2.2.2 Pre-deposition Preparation

2.2.2.1 Flow Rate Calibration

The volatile liquid precursor is transported by pushing it with nitrogen pressure from the container to the reactor. Flow rate control for the reactant was established by the relationship (Flow Rate = $K \cdot \text{Pressure}_{\text{gauge}}$), where K is constant and the units for flow rate

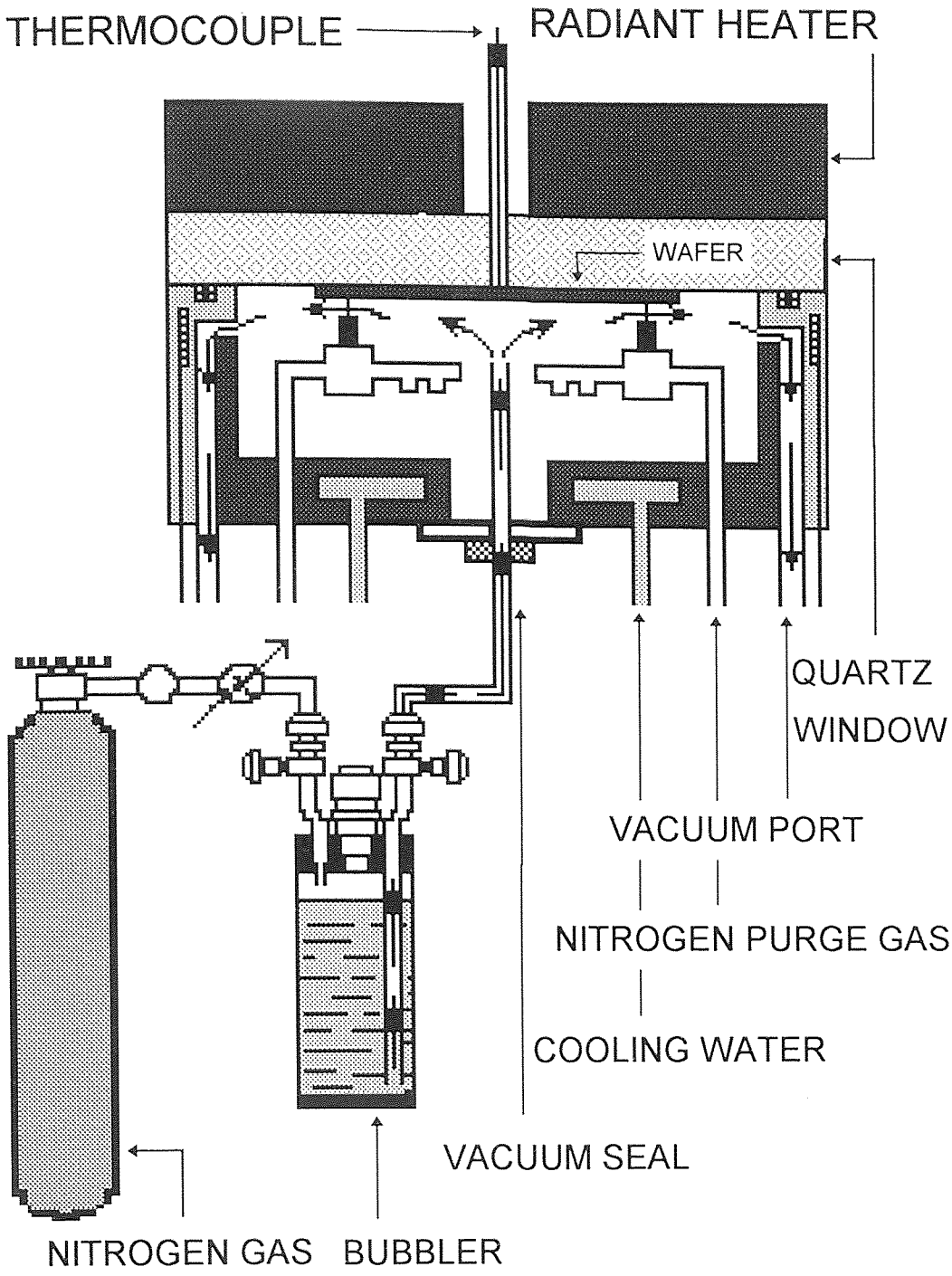

Figure 2.1 Schematic of experimental set-up.

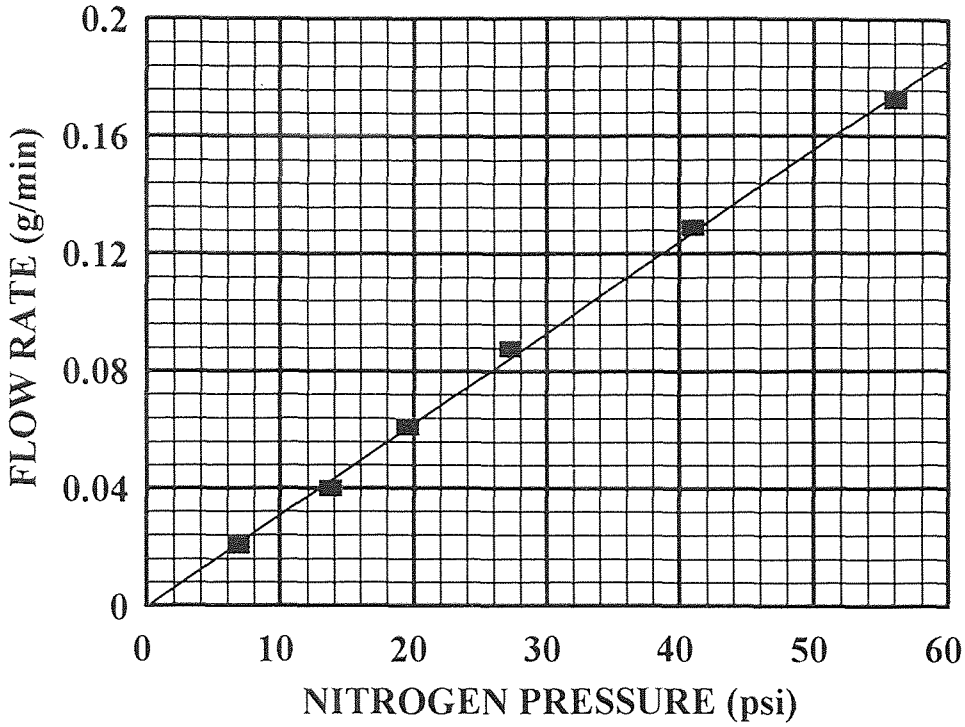

Figure 2.2 The flow rate of Cu complex precursor as a function of nitrogen pressure through a capillary tubes 5m, ID 0.01", OD 1/16".

The flow rate calibration procedure was accomplished in a open reactor. The procedure was as follows: (1) weigh an empty small glass bottle as a precursor container, (2) set the nitrogen pressure to a certain set point, (3) open the shut-off valve (start the reactant flow) and let the liquid precursor flow into the glass bottle, (4) after a certain period of time, turn off the shut-off valve (stop the reactant flow) and weigh the bottle again, in order to calculate the weight difference (weight of liquid precursor) to determine flow rate, (5) calculate the gauge pressure. Therefore, several sets of data can be obtained as shown in Figure 2.2.

2.2.2.2 Leak Check

A leak check was conducted before beginning of any experimental run to avoid oxygen and ensure formation of films with desirable and reproducible quality. For the SPECTRUM CVD 211, most experimental conditions (except Cu(I)(hfac)(tmvs) precursor flow rate) can be read directly from the monitor; therefore, during this leak check procedure, the reactor was closed, connected to a vacuum system, and the pressure decreased to near zero. This process takes several seconds.

2.2.3 Operation Procedure

2.2.3.1 Wafer Transport

All wafers were marked first and weighed accurately to 0.1 mg before and after deposition. In this system 10 cm diameter single crystal <100> silicon wafers are loaded through a load-lock by a casette-to-casette transport facility. The whole wafer transport was carried out by automatical control of the machine, and the whole operation process also can be controlled from the monitor.

2.2.3.2 Film Deposition

The film deposition is achieved in five steps process: (1) a ramp step (increasing the reactor temperature rapidly from room temperature to set point (140 to 250 °C), (2) a bake step (start purge nitrogen to keep the reactor temperature at approximately the set point), (3) a deposition step, (4) a pump down step (removing all the precursor from the reactor), (5) a cooling down step (decrease the wafer temperature with nitrogen gas until

the wafer temperature below 100 °C). The reactor wall were maintained at 50 °C by using cooling water at that temperature. During deposition the flow rate and the temperature were held constant while the reactor pressure was kept in a small range around the set point by the throttle valve.

2.3 The Chemistry of Copper CVD

2.3.1 Precursor Chemistry

The desirable characteristics of metal CVD precursors must possess thermal stability and adequate volatility, decompose to high purity metal. The physicochemical properties of the precursor play a critical role in the CVD process because they determine (1) vapor pressure, (2) the behaviors of adsorption and desorption, (3) the purity of the deposited metal, (4) the deposition rate of thin film, and (5) the decomposition temperature. These combined chemical and physical properties are a direct result of the precursor molecular structure. CVD precursors must have the following properties,

(1) They must be either gases or liquids with a high vapor pressure at room temperature.

(2) The decomposition temperature must be lower than the deposition temperature.

(3) The evaporation temperature must be lower than the decomposition temperature.

(4) The vapor pressure must be higher than the reaction pressure.

(5) There must be no carbon, oxygen, or any other impurity mixed with the copper contained in the precursor during the copper deposition.

(6) Stable transfer of precursor vapors should be possible [31].

The pure copper films are deposited from the Cu(I)(hfac)(tmvs) precursor, which belongs to the ligand-stabilized Cu(I)β-diketonate family, by the process of thermally induced disproportionation reaction.

$$2Cu(I)(hfac)(tmvs) \Rightarrow Cu(0) + Cu(II)(hfac)_2 + 2(tmvs)$$

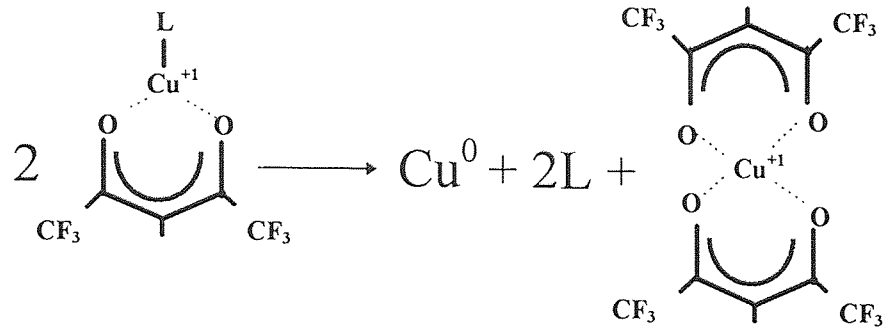

L(ligand): Trimethyl Vinylsilane.

Figure 2.3 The disproportionation reaction of Cu(I)(hfac)(tmvs).

When the Cu precursor molecule is adsorbed on the surface the (tmvs) ligand is removed generating two unstable Cu(I)(hfac) molecules which disproportionate into a metallic Cu and a volatile Cu(II)$(hfac)_2$ molecule. Since the ligand is weakly bound in the complex, the thermal decomposition of these complex occurs at low temperature (150°C to 250°C) and result in the formation of a near bulk copper film. The mechanism for heterogeneous decomposition are shown as above.

The chemical and physical properties of precursor can be changed by altering the chemical structure of the precursor via substitution of different Lewis-base ligands or different β-diketonates. The modification of the chemical structure of the precursor can

directly change the physical state (liquid or solid), the partial pressure, the decomposition temperature and long-term stability of the copper precursor [5].

2.3.2 CVD Reaction Chemistry

Several possible mechanisms for copper deposition reaction have been proposed. The heterogeneous surface reaction by Langmuir-Hinshelwood reaction for an example. Heterogeneous surface reactions involving one molecular of a reactant can be treated by Langmuir adsorption isotherm [25,26]. Let θ be the fraction of surface that is covered and $(1-\theta)$ the fraction that is bare. The rate of adsorption is then $k_1 p(1-\theta)$, where p is the gas pressure and k_1 is proportionality constant, the rate of desorption is $k_{-1}\theta$. At steady state, the rates of adsorption and desorption are equal , so that

$$\frac{\theta}{1-\theta} = \frac{k_1}{k_{-1}} p = Kp \qquad (2.1)$$

where K, equal to k_1/k_{-1}, is the adsorption equilibrium constant. This equation can be written as

$$\theta = \frac{Kp}{1+Kp}, \qquad (2.2)$$

The rate of reaction is proportional to θ and may therefore be written as

$$Deposition\ \ Rate = k_2\theta = \frac{k_2 Kp}{1+Kp} = k_0 \cdot e^{\frac{-Ea}{R \cdot T}} \cdot \frac{Kp}{1+Kp} \qquad (2.3)$$

where k_2 is the proportionality constant. This is the simplest treatment of surface reaction. However, in many cases, surface reactions between two substances follow a bimolecular surface reaction model. Two adjacent sites must be occupied by reactant molecules. The rate of reaction is proportional to θ^2 and may therefore be written as

$$Deposition\ \ Rate = k_2\theta^2 = A \cdot e^{\frac{-Ea}{K \cdot T}} \cdot \left(\frac{Kp}{1+Kp}\right)^2, \qquad (2.4)$$

2.3.3 Growth Chemistry

For CVD copper metallization, the conductivity and catalytic nature of the substrate dictate the initial growth behavior. The growth behavior can be divided into two different kinds as follows. First, as shown in Figure 2.4, deposition can take place on an activated inert nonconducting substrate and form small copper islands. These islands then act as growth centers from which the initial copper spheres will enlarge and grow hemispherically before they finally merge into one continuous film.

Second, if the substrate is conducting, the conductivity helps to spread the cathodic regions. Therefore, on an activated inert conducting substrate, deposition can occur on the entire substrate surface, instead of only on the inert nuclei. The catalytic particles serve mainly as the anodic sites at which the reductant molecules are adsorbed and oxidized as shown in Figure 2.5 [27].

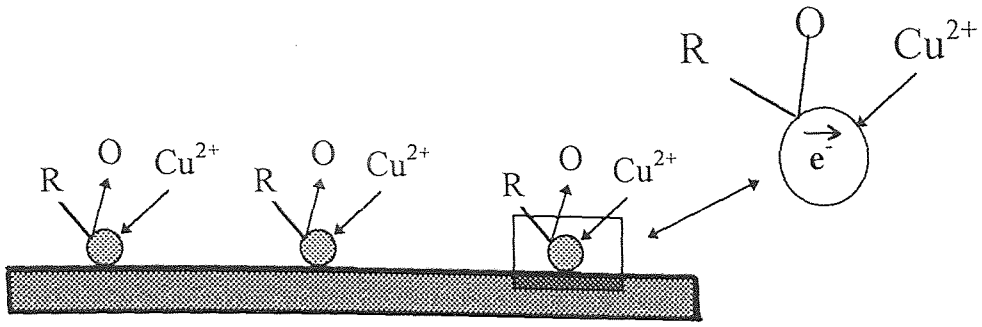

R=Reductant O=Oxidized form of Reductant

Figure 2.4 Activated inert non-conducting substrate.

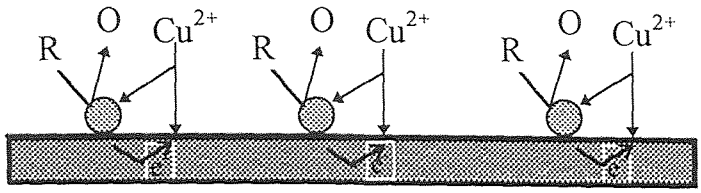

R=Reductant O=Oxidized form of Reductant

Figure 2.5 Activated inert conducting substrate.

2.4 Copper Film Characterization Techniques

2.4.1 Physical Properties

The thickness measurement was accomplished by Dektak. The measurement procedure includes two steps: (1) peeling the copper film with scotch tape as close as possible to the center of the wafer, (2) measuring the height difference between the copper film surface (unpeeled part) and silicon substrate (peeled part) by using Dektak's carbon pin moving across these two areas. As shown in Figure 2.6, the profile of Dektak thickness measurement can be divided into two area and in the meddle, the highest peak, was caused

by peeling. The higher part is the copper film and the lower one is silicon substrate. Density of the CVD copper films was determined from the slope of the plot of film thickness versus film mass.

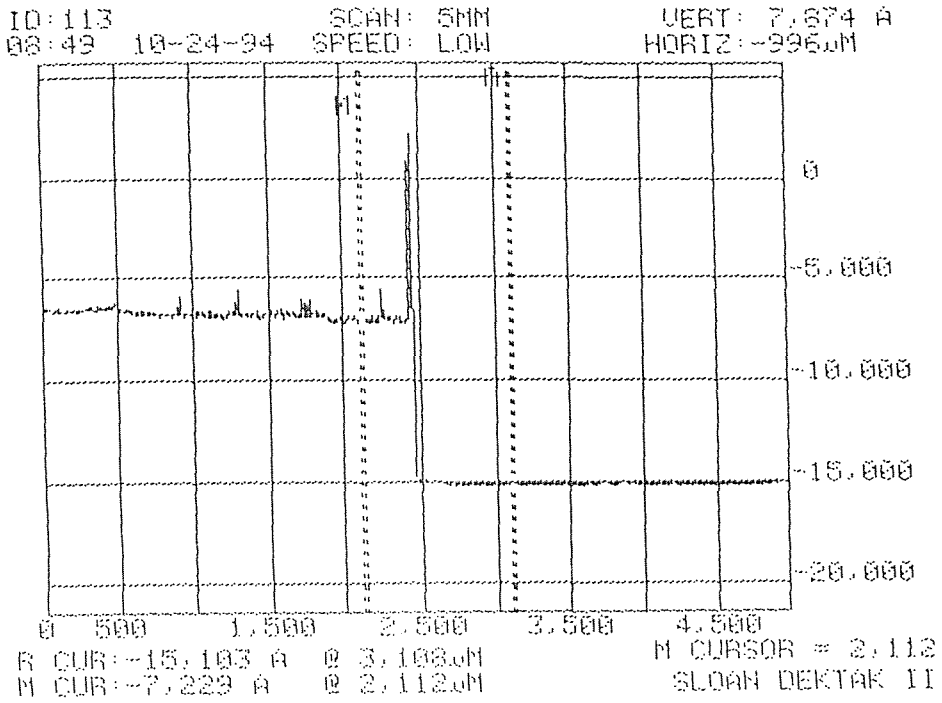

Figure 2.6 The profile of Dektak thickness measurement.

2.4.2 Electrical Properties

Four-point probe method is the most common technique to measure the sheet resistance. The process is outlined in Figure 2.7. The electrical resistance R of a rectangularly shaped section of thin film with length L, width W, and thickness D, is given by

$$R = \rho \frac{L}{D \times W}$$

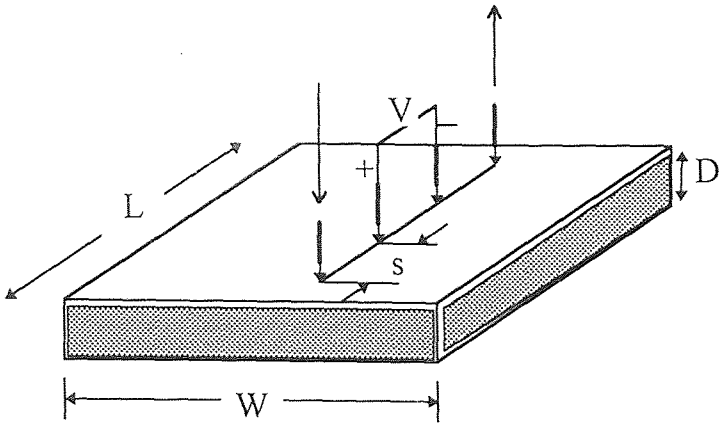

Figure 2.7 Four-point probe system for sheet resistance measurement.

where ρ is the resistivity of the material. If L = W, the equation shown as above becomes

$$R = \frac{\rho}{D} = R_s$$

where R_s is called the sheet resistance and is expressed in Ω/□, therefore from the sheet resistance and thickness, the resistivity can be obtained.

2.4.3 Compositional Properties

The elemental composition and chemical states were studied by X-ray Photoelectron Spectroscopy (XPS), Auger Electron Spectroscopy (AES) and Rutherford Backscattering Spectrometry (RBS) measurements.

In the XPS measurement, low energy X-ray such as K_α X-ray of unmonochromatized aluminum at the energy level of 1.487 Kev, 250W were employed to

bombard the sample and cause photoelectron emission. The X-ray photo energy removes an inner shell electron from an atom when it is absorbed. The electron is emitted with a kinetic energy characteristic of the difference between the X-ray and the binding energy of the electron. This energy of the emitted electron can be used to determine the type of the atom, and the number of such a electrons with this energy is related to the number of atoms present. XPS, shown in Figure 2.8, can be used to examine several top monolayers of thin film and provide information about the chemical bonding of the elements. The limitation of the XPS is that it can not detect hydrogen and helium since the XPS measurement process involving the excitation and emission of at least three electrons [29].

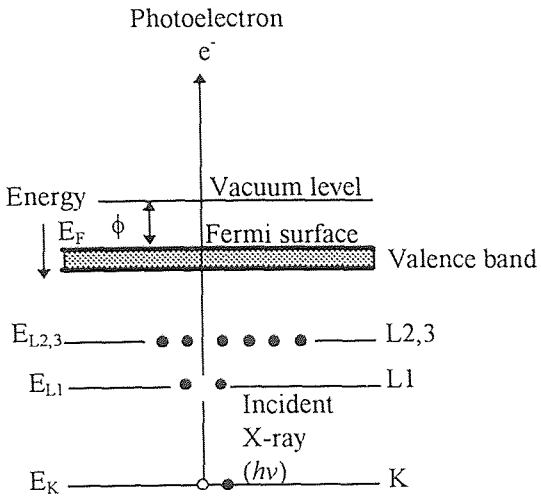

Figure 2.8 The energy diagram of X-ray Photoelectron Spectroscopy (XPS).

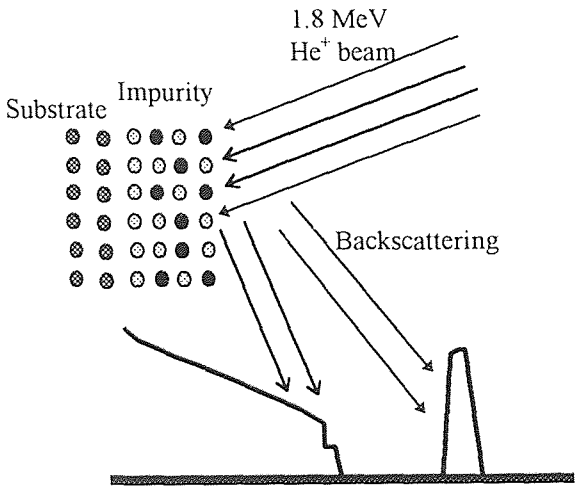

Figure 2.9 The principle of Rutherford Backscattering Spectrum (RBS).

The Rutherford Backscattering Spectroscopy (RBS), shown in Figure 2.9, measurements were taken using a High Voltage Engineering AK accelerator with He^+ ions

at an energy of 1.8 Mev to corroborate the XPS data. Scattering techniques are often used in atomic and nuclear physics to check targets for impurities, thickness and composition. Energy transfer by elastic collisions from a projectile to a target atom can be calculated from collision kinematics and the probability of elastic collision between the projectile and target atom is highly predictable [29]. Therefore, the quantitative analysis of atomic composition can be obtained by the scattering probability or scattering cross section.

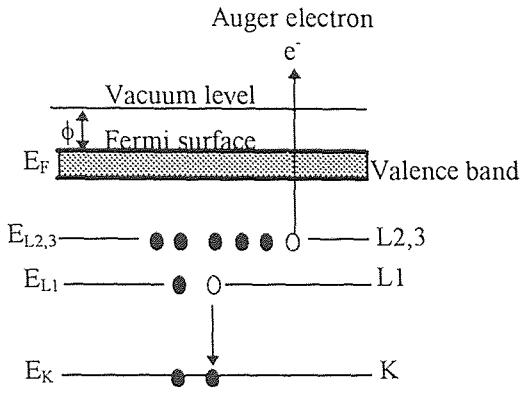

Figure 2.10 The energy diagram of Auger Electron Spectroscopy (AES).

Auger electron spectroscopy (AES), shown in Figure 2.10, is the most widely used surface-sensitive analytical techniques capable of providing elemental composition of the outermost atomic layer of a solid. This techniques can be used to investigate the surface chemistry and interactions of solid surface. Therefore, from the ratio of these peaks from AES spectrum, the purity of CVD copper film can be assured.

2.4.4 Structure Properties

The crystallographic orientation of the CVD copper film was established by X-ray diffraction measurements using with a Cu target on a Rigaku DMAX II system operating at 30 KV and 20 mA. Optical microscopy was used to inspect for the possible presence of cracks, gas phase nucleation clusters, and other defects in the deposits [29] as shown in Figure 2.11.

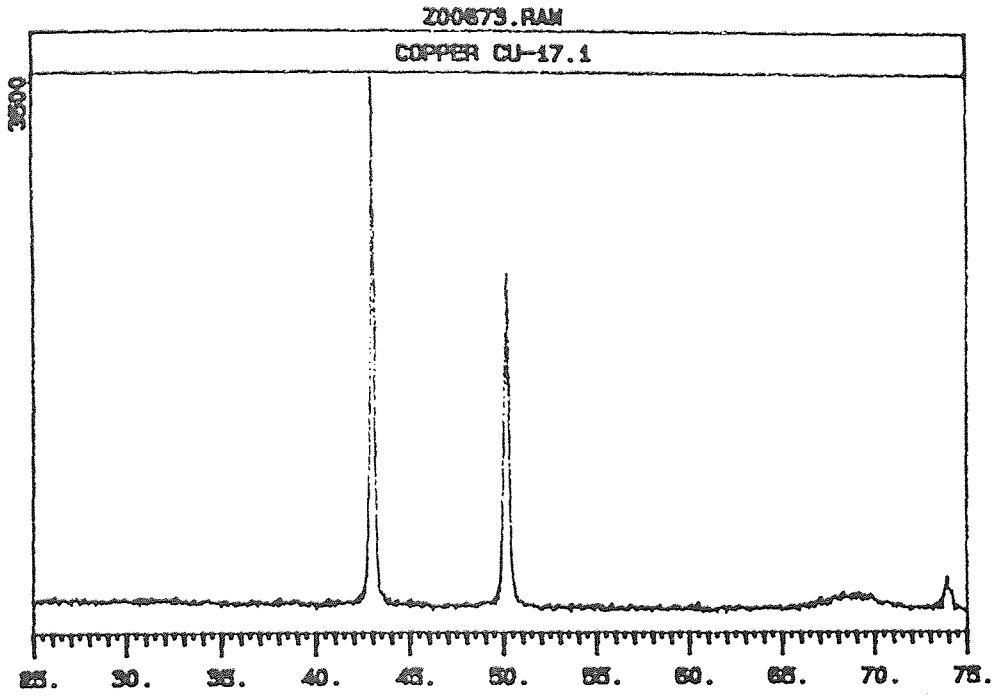

Figure 2.11 The spectrum of X-Ray Diffraction (XRD).

A primary use of the scanning electron microscope (SEM) is to produce high-resolution and depth-of-field images of sample surfaces and can provide chemical analysis of micron-sized areas of the structure revealed on these surfaces and almost same as the

Atomic Force microscope (AFM) [29] which also can provide the surface morphology by measuring the repulsive force. The transmission electron microscopy (TEM) [29] can simultaneous examine the microstructural features through high-resolution imaging, and the acquisition of chemical and crystallographic information from small (submicrometer) regions of the specimen. Therefore, these measurements can offer very important information about film roughness, surface morphology, film orientation, purity, grain shape and size for the further understanding of CVD copper film.

CHAPTER 3

RESULTS AND DISCUSSION

3.1 The Effects of Deposition Variables on Film Deposition Rate and Film Composition

3.1.1 Temperature Dependent Study

The temperature dependent behavior of deposition rate is shown in Figure 3.1 for the conditions of a constant Cu(I)(hfac)(tmvs) precursor flow rate (7.85 sccm) and the total reactor pressure (100 mTorr). The deposition reaction seems to follow an Arrhenius type behavior in the temperature range from 150 °C to 180 °C with the growth rate increasing up to a deposition temperature of 220 °C, followed a slightly decrease when the temperature reached 250 °C. The whole reaction behaviors (in the temperature range from 150 to 250 °C) observed are similar to the model of temperature dependent behavior of CVD reaction shown in Figure 1.5. An activation energy of about 16 kcal/mole was calculated from the slope in the region where Arrhenius behavior was observed (150-180 °C) by using a linear regression analysis to the following equation:

$$\text{Growth Rate} = k_0 \times e^{\frac{-Ea}{k \cdot T}}.$$

This result is comparable to the value of 13 kcal/mole reported for copper films synthesized from Cu(I)(hfac)(tmvs) precursor [12].

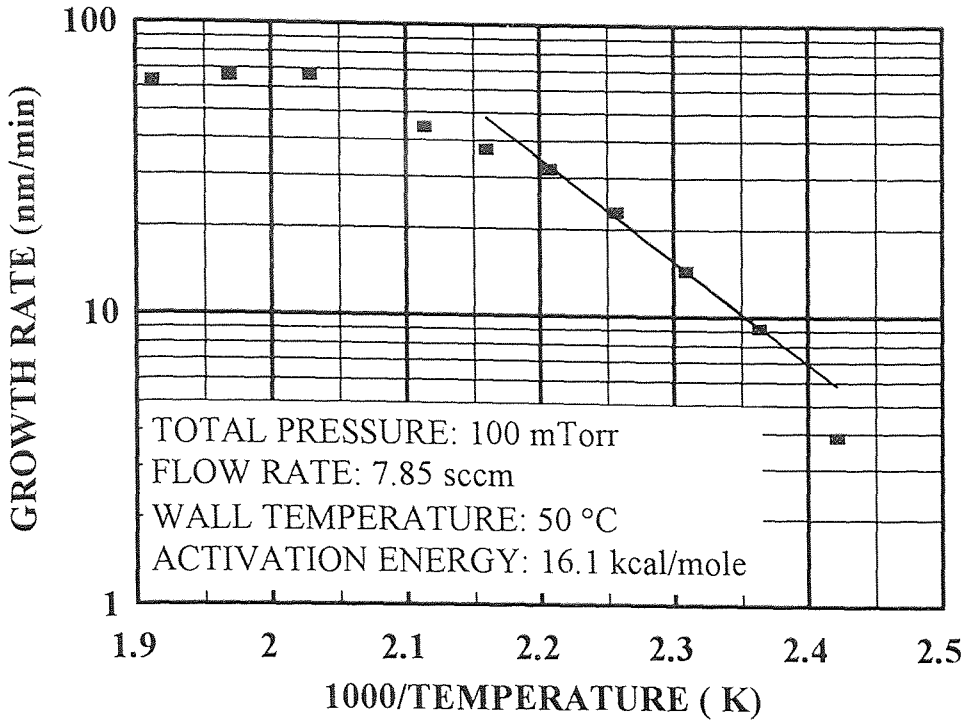

Figure 3.1 Dependence of growth rate on temperature.

Two interesting phenomena were found in this experiment. First, when the temperature is higher than 220 °C, the adhesion of copper film to silicon substrate starts to decrease , and when the temperature is higher than 250 °C, the copper film does not stick to the silicon substrate (the film just float superficially on the silicon substrate). To explain this problem two assumptions were offered. (1) the substrate is not thoroughly clean in the deposition reaction. This is not only because impurities on the surface can physically block the deposition of a copper film and so lead to a discontinuous, flaky layer, but also because they can markedly affect the mode and amount of nucleation of the depositing material. However, after comparing with these deposited films, it shows that the degree of adhesion was inversely proportional to growth temperature, therefore, another

hypothesis (2) was made that the interfacial transition zone, a new phase between the layer and the substrate, was formed. Sometimes an interfacial zone is formed by interdiffusion of the copper and substrate materials so that there is a buffer region with properties intermediate between the copper and substrate; within this "buffer" region, stresses caused by mismatch of crystallographic parameters, differences in thermal expansion coefficients and microstructural defects, can be released [17].

The second interesting phenomenon is that at a lowest temperature, 140 °C, the growth rate of the deposited film deviated from the Arrhenius behavior. This phenomenon has occurred twice for the same type of experiment with different reaction conditions. The reason for the behavior of the 140 °C point resulted from the precursor Cu(I)(hfac)(tmvs) chemistry mentioned in chapter 2, since the Lewis-base ligand (trimethylvinylsilane) is weakly bound in the copper complex Cu(I)(hfac)(tmvs), the thermal decomposition of this copper complex occurred at low temperatures (150-250 °C) [4,6] and resulted in the formation of near-bulk copper films. Therefore, when the growth temperature is lower than 150 °C, an incomplete decomposition reaction of the Lewis-base ligand (tmvs) occurred, so that the probability of the disproportionation reaction decreased and caused the 140 °C point to have an non Arrhenius behavior was due to the decreased growth rate.

3.1.2 Pressure Dependent Study

The pressure dependent behavior of deposition rate is shown in Figure 3.2, with the condition of a constant Cu(I)(hfac)(tmvs) precursor flow rate (7.85 sccm) and a constant

growth temperature (180 °C). The deposition rate was found to increase in the low pressure range of 50 to 100 mTorr followed by a constant deposition rate (indicating that a saturation was reached). As the total pressure increased, more gaseous reactants were adsorbed on the substrate surface and more sites were occupied by the reactant molecules. Thus, more of the available surface area is occupied, and the deposition rate increased. However, as the pressure increased above 100 mTorr, a zero-order pressure dependence [30] was observed, because the surface can always become saturated with the adsorbed species saturating the coverage. Thus the reaction rate is constant and becomes insensitive to the adsorption and desorption kinetics.

Since the low pressure control of the SPECTRUM CVD 211 is difficult, a higher precursor flow rate was necessary for this experiment in order to ensure an accurate model for the pressure dependency as observed Figure 3.2. Since a non-linear behavior was observed, two different flow rate were used in the 0 - 100 mTorr region. Both of these studies could be explained by a second-order adsorption kinetics, i.e., rate of adsorption = $k_d[P_x(1-\theta)]^2$, and the rate of desorption = $k_{-d}\theta^2$. Then there are conditions that exhibit an half order pressure dependence behavior [30], as shown in Figure 3.3. This behavior can be prove by following equations:

$$At\ steady\ state:\ k_d \cdot (p_x(1-\theta))^2 = k_{-d} \cdot \theta^2$$

$$\left(\frac{k_d \cdot p}{k_{-d}}\right)^{\frac{1}{2}} = \frac{\theta}{1-\theta}, \quad so\ \theta = \frac{\left(\frac{k_d \cdot p}{k_{-d}}\right)^{\frac{1}{2}}}{1+\left(\frac{k_d \cdot p}{k_{-d}}\right)^{\frac{1}{2}}}$$

$$Deposition\ Rate = k_0 \cdot e^{(-Ea/kT)} \cdot \theta$$

$$= k_0 \cdot e^{(-Ea/kT)} \cdot \frac{\left(\frac{k_d \cdot p}{k_{-d}}\right)^{\frac{1}{2}}}{1+\left(\frac{k_d \cdot p}{k_{-d}}\right)^{\frac{1}{2}}}$$

When the total pressure is low, the square of θ is proportional to the precursor partial pressure, so that the half-order pressure dependence behavior is quite sure, and simulation lines were also shown in Figure 3.4.

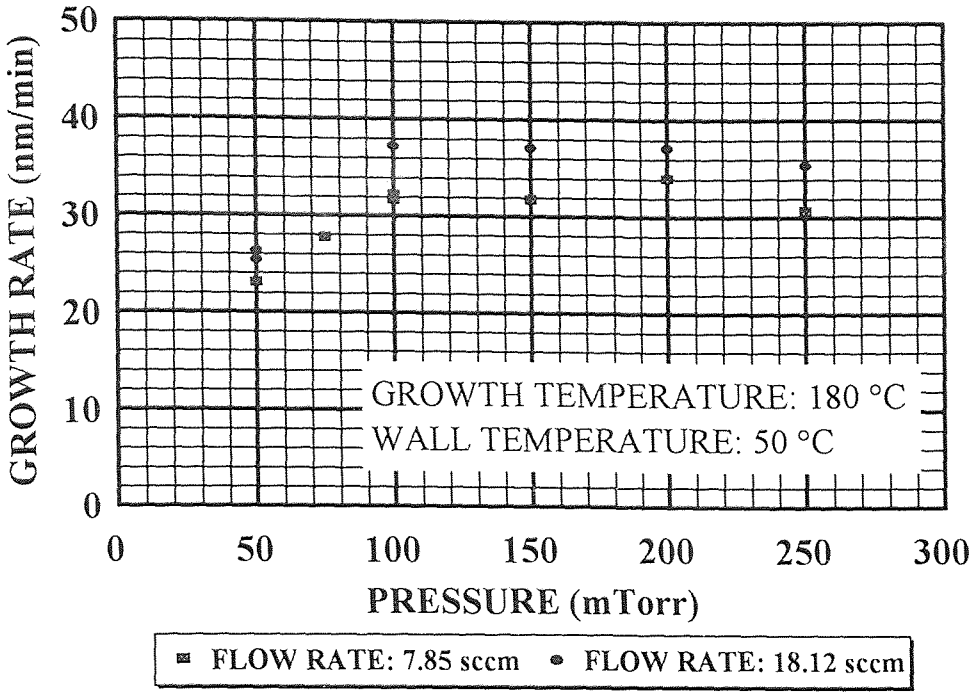

Figure 3.2 Dependence of growth rate on total pressure.

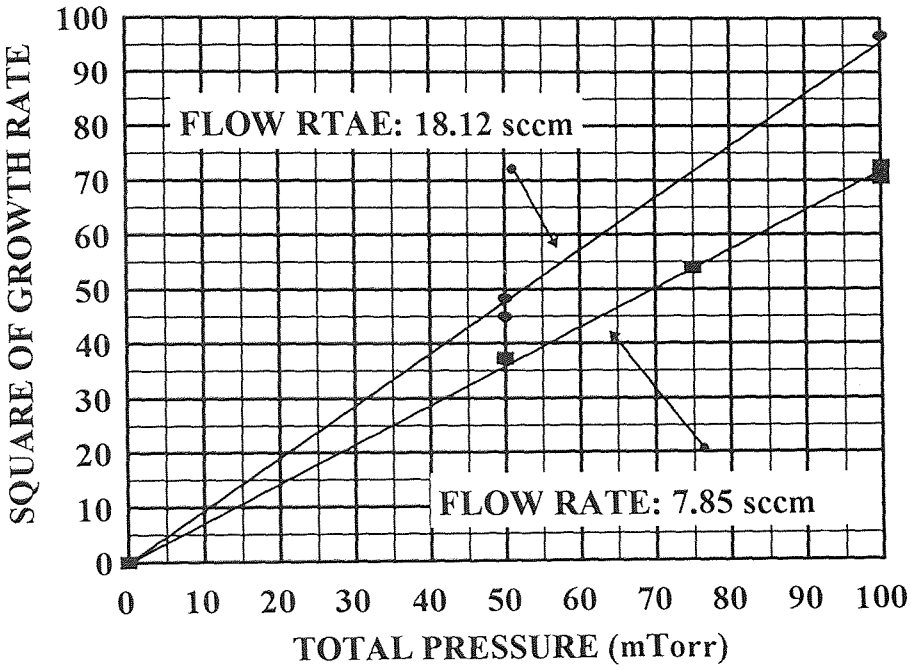

Figure 3.3 Dependence of square of growth rate on total pressure.

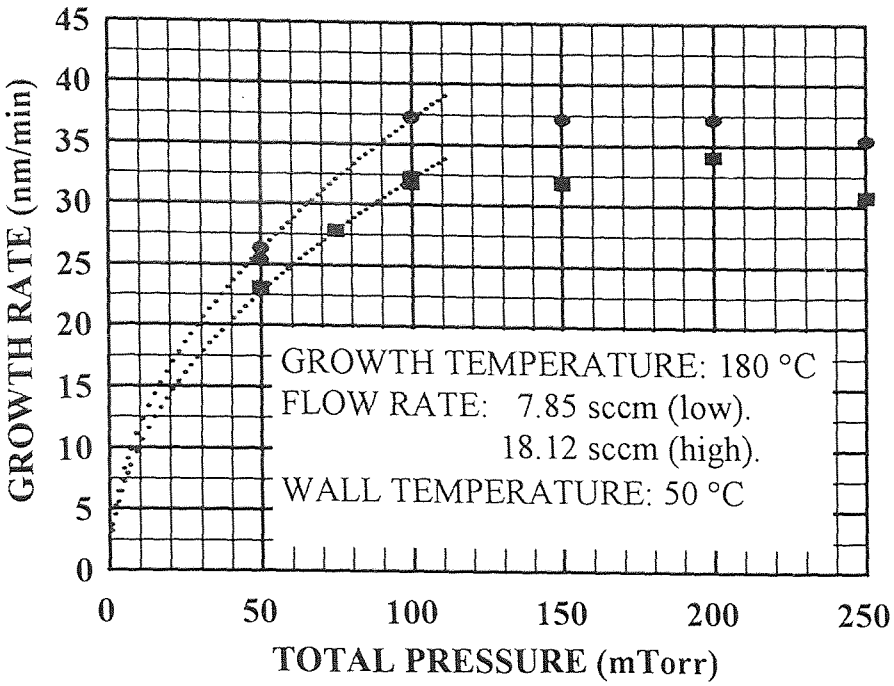

Figure 3.4 Simulation lines of the half-order pressure dependence behavior (square of growth rate versus to total pressure).

3.1.3 Flow Rate Dependent Study

The flow rate dependent behavior of deposition rate is shown in Figure 3.5, for conditions of constant growth temperature (180 °C) and constant total pressure (100 mTorr). The deposition rate was found to increase in a non-linear manner in the low flow rate regime (below 6.04 sccm) followed by saturation above flow rate of 12.08 sccm. The flow rate dependency can be explained by the fact that an increase of the precursor, Cu(I)(hfac)(tmvs), flow rate results in an increase in the pumping out of by-product to maintain a constant pressure. Therefore, the partial pressure of unreacted precusor increases and the growth rate increases. This increase follows the same model as with a pressure increase (see Figure 3.6 and Figure 3.7).

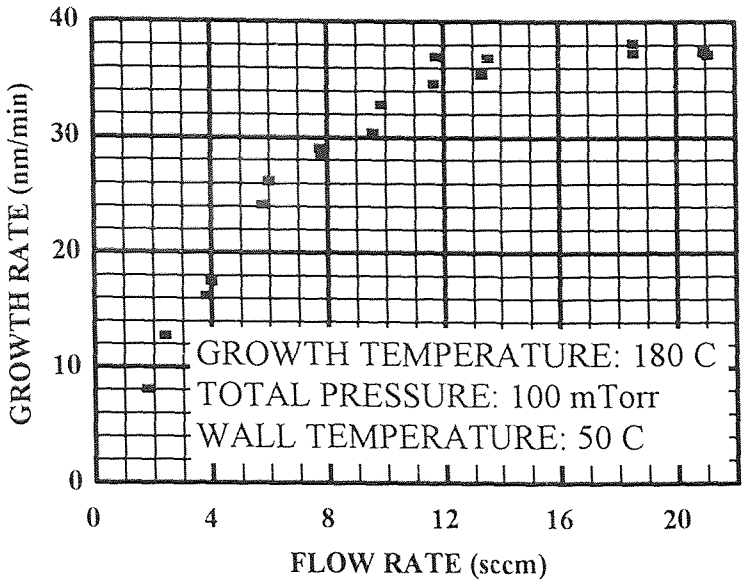

Figure 3.5 Dependence of growth rate on precursor flow rate.

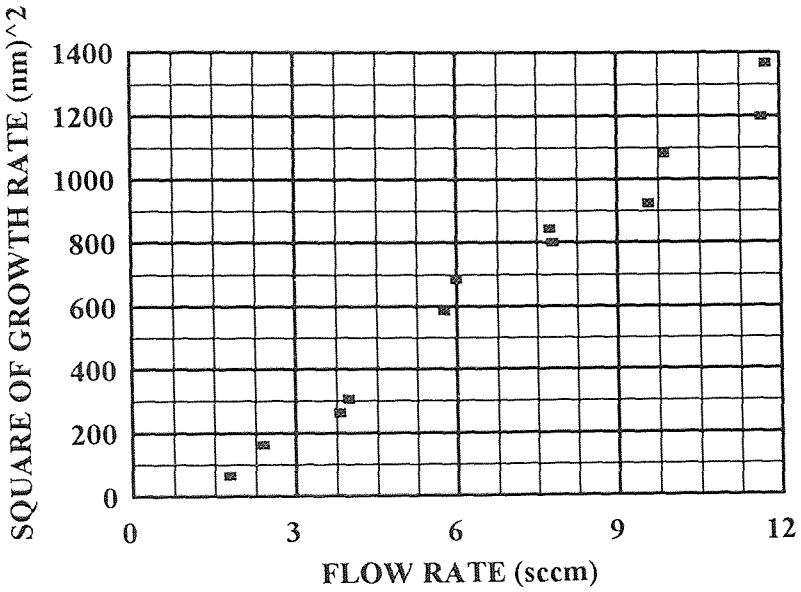

Figure 3.6 Dependence of square of growth rate on precursor flow rate.

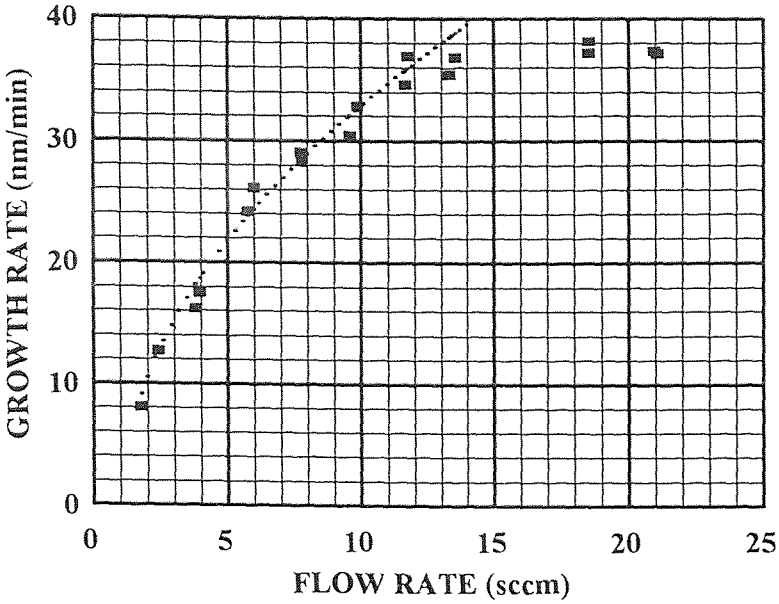

Figure 3.7 Simulation lines for the half-order flow rate dependence behavior (square of growth rate versus to precursor flow rate.).

3.2 Copper Film Characteristics

3.2.1 Purity

The purity of the deposited film is very important aspect for CVD copper deposition. In these experiments, the purity of films deposited standard condition (growth temperature 180 °C, flow rate 7.85 sccm and total pressure 100 mTorr) were analyzed by AES (Auger Electron Spectroscopy), XPS (X-ray Photon Spectroscopy), and RBS (Ruthford Backscattering Spectroscopy). The results of XPS measurements demonstrated that the deposited copper films had a very thin surface impurity covering which was removed by the 2 nm argon etch. This coating was a mix of Cu, CuO, and Cu_2O, and adsorbed organics. Even after just 2 nm etching, the Cu Auger peak shows only a few percent

oxide with the rest of the signal being metallic copper. After 12 nm etch, even this small amount of oxide is removed.. The Auger spectrum, which is the most sensitive probe of copper oxidation, was here indistinguishable from a thoroughly etched pure metal foil. The very small carbon signal is just neutral carbon, graphite-like.

From Auger depth profile, the atomic concentrations of the copper, oxygen, carbon were monitored as a function of sputtering time. Any impurity on the surface disappeared rapidly below the detection limit as the depth profiling proceeded. The XPS spectra and the sputter depth XPS profile are shown in Figure 3.8 to Figure 3.10. These results were confirmed with RBS measurement as shows in Fig 3.11.

3.2.2 Resistivity

The main reason that copper is believed to be the most promising candidate for on-chip interconnection in the upper-level metallization is its low bulk electrical resistivity. This low resistivity can allow higher current density to be imposed on copper wiring with a smaller line width, minimized interconnection or RC time delay of the device. The electrical resistivity of deposited copper films was obtained from the four point probes sheet resistance measurement and Dektak thickness measurement. The function of the sheet resistance are show as follows:

$$Sheet\ Resistance\ (\Omega/\square) = \frac{Resistivity(\Omega \cdot cm)}{Thickness(cm)}.$$

The sheet resistance data of the copper films which were deposited at various deposition conditions as a function of film thickness are shown in Figure 3.12. The electrical resistivity of the deposited film is strongly related to the film thickness, as shown in Figure 3.13, with the higher resistivity shown in thin films (thickness < 0.5 μm) due to electron scattering effects [7], as seen in other CVD metallization reaction.

In order to explain the resistivity further, three operation parameters are considered to be variables for the resistivity studies. The three studies are based on the standard reaction condition (growth temperature 180 °C, total pressure 100 mTorr, and precursor flow rate 7.85 sccm), The range for these parameters were varied from 140 °C to 235 °C for the temperature series, from 50 to 250 mTorr for the pressure series and from 2.41 to 21.08 sccm for the precursor flow rate series. These results ar shown from Figure 3.14

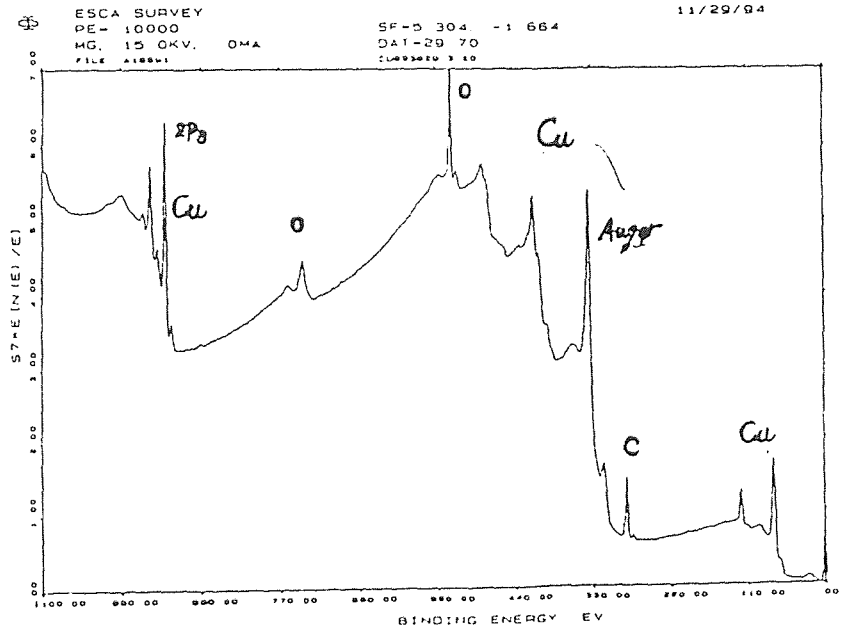

Figure 3.8 XPS spectrum of the deposited CVD film (on surface). The deposition condition 180 °C, 100 mTorr, and precursor flow rate 7.85 sccm.

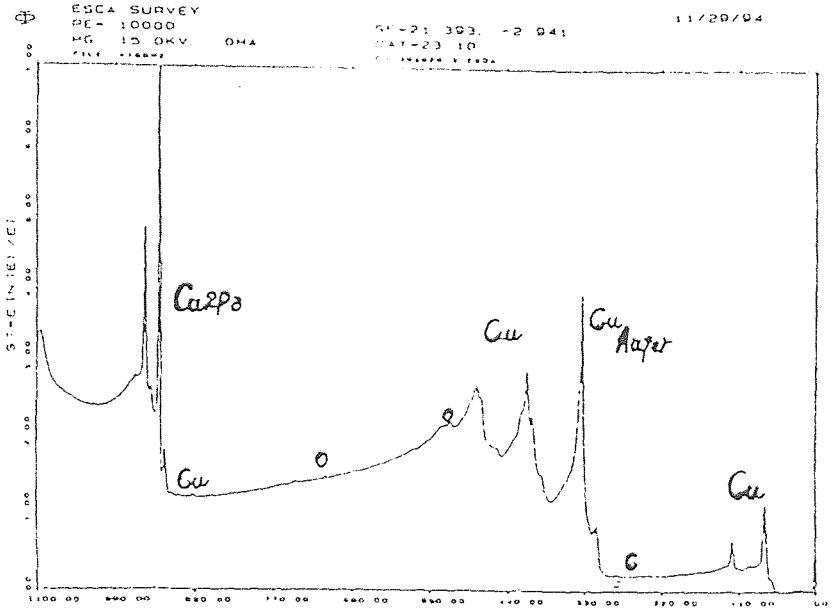

Figure 3.9 XPS spectrum of the deposited CVD Cu film after sputter cleaning of the film surface, approximately 2 nm. The deposition condition 180 °C, 100 mTorr, and precursor flow rate 7.85 sccm.

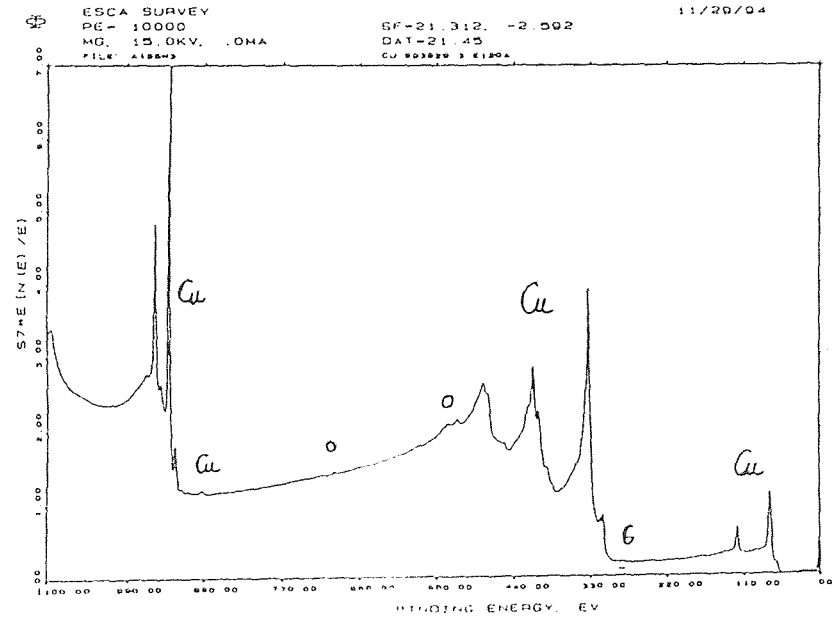

Figure 3.10 XPS spectrum of the deposited CVD Cu film after sputter cleaning of the film surface, approximately 12 nm. The deposition condition 180 °C, 100 mTorr, and precursor flow rate 7.85 sccm.

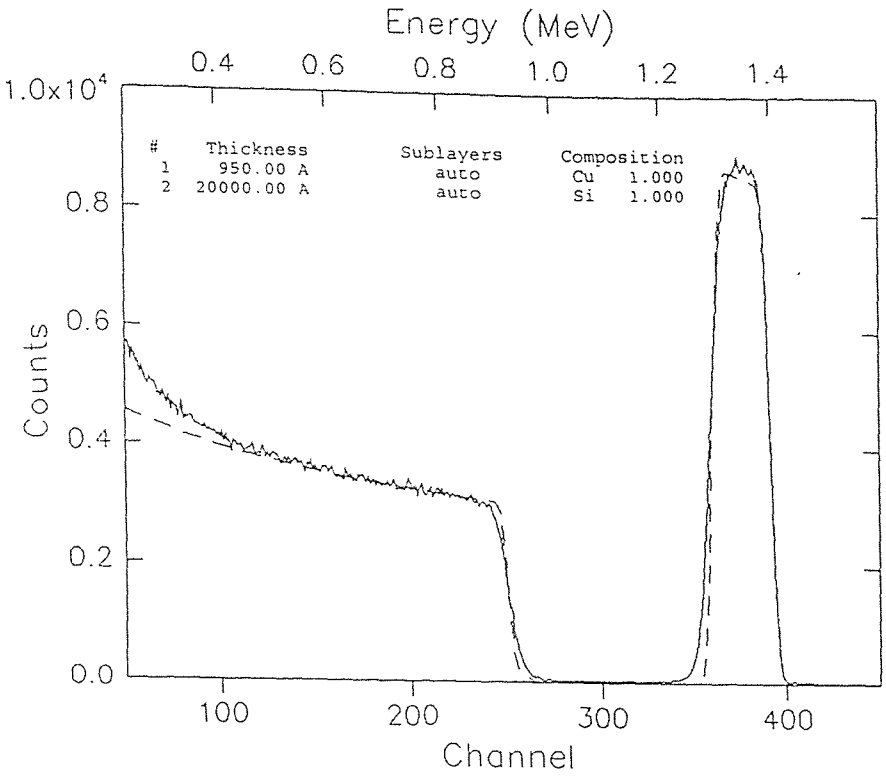

Figure 3.11 RBS spectrum of the deposited CVD Cu film. The deposition condition 180 °C, 100mTorr, and precursor flow rate 7.85 sccm.

to Figure 3.16, and it is clear that the measured resistivity varies in a small range between 2.1 to 2.3 ($\Omega \cdot$ cm) for both pressure and flow rate study series. The independent behaviors of pressure (50-250Torr) series and flow rate (2.41-21.08 sccm) series can be determined. However, in temperature study series, shown in Figure 3.16, the values of resistivity seems to increase as the deposition temperature increased from 170 °C to 140 °C. The poorly connected grains of the structure [1,3] and the electron scattering effect [11] caused by phonons, impurities, vacancies, dislocations, grain boundaries, precipitated second phase particles, and compound phase [14] may be used as an explanations for these behaviors.

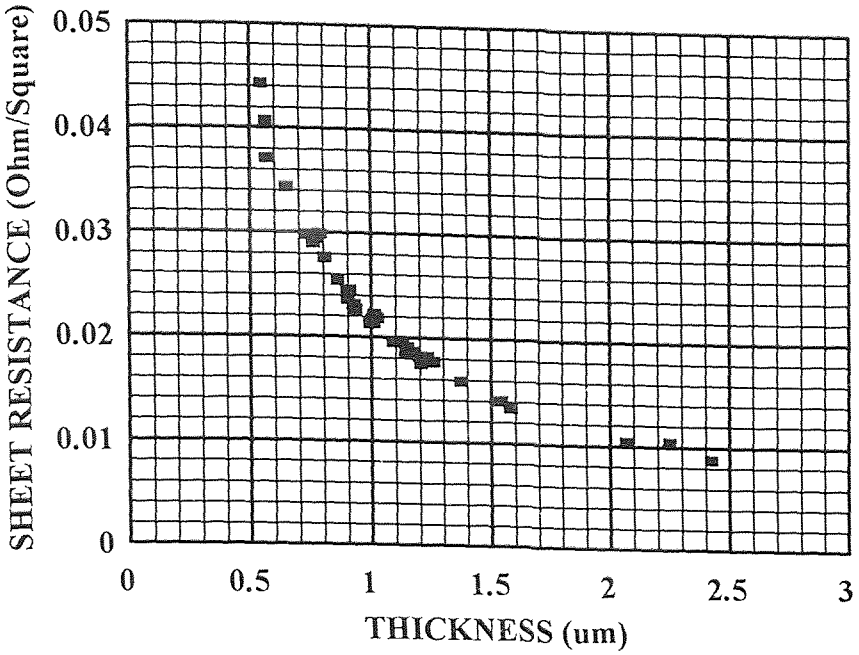

Figure 3.12 Sheet resistance of CVD Cu as a function of film thickness.

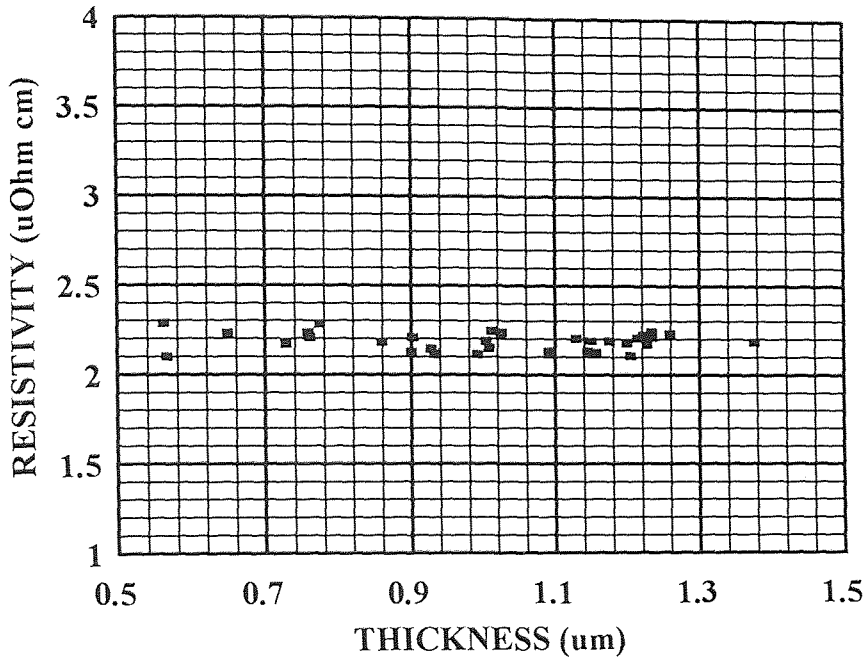

Figure 3.13 The average value of resistivity of CVD Cu was 2.2 (μOhm×cm) for a series data with different deposition reaction condition.

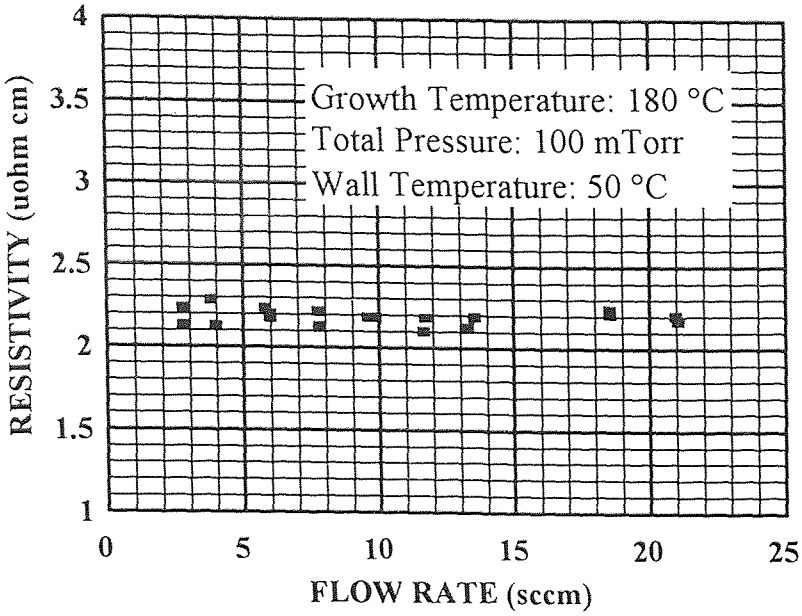

Figure 3.14 The independent behavior of resistivity of CVD Cu on precursor flow rate.

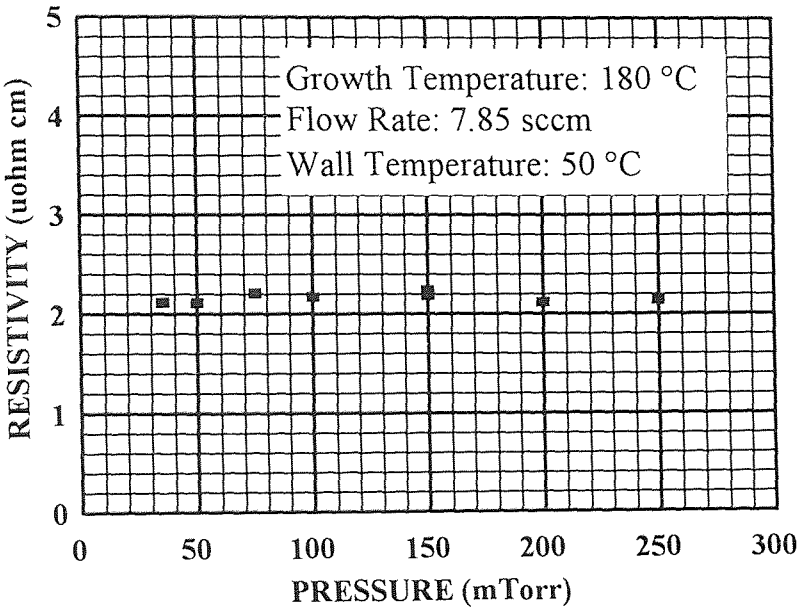

Figure 3.15 The independent behavior of resistivity of CVD Cu on total pressure.

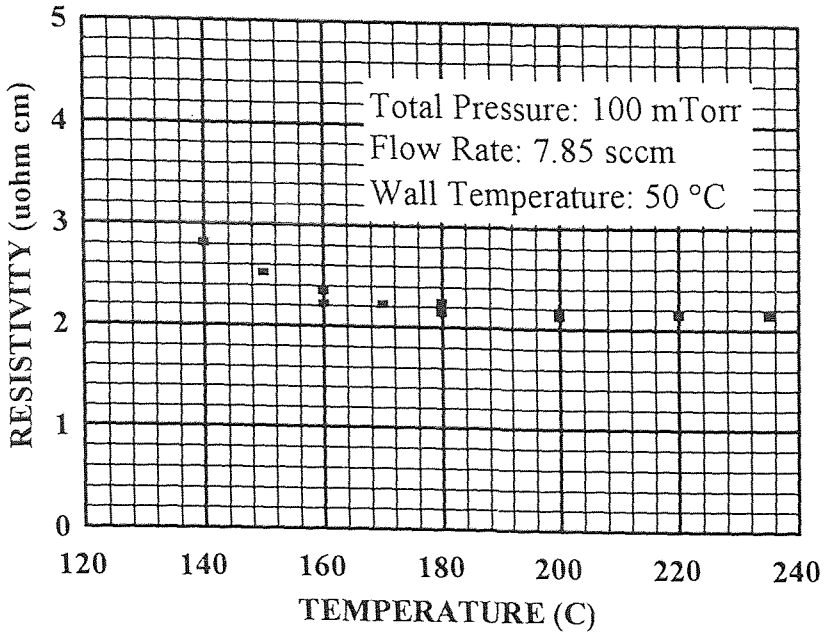

Figure 3.16 The dependent behavior of resistivity of CVD Cu on temperature.

3.2.3 Surface Morphology

Scanning electron microscopy (SEM), atomic force microscopy (AFM), transmission electron microscopy (TEM) were used to study the effects of deposited film surface morphology (brightness, surface roughness) and the variation of surface morphology with film thickness. The AFM and SEM photos as shown in Figure 3.17 and Figure 3.18 demonstrate the average and maximum of surface roughness of deposited copper films with the same deposition condition but different thickness. These results are reinforced in a comparison between the AFM and SEM measurements, establishing that the surface roughness is proportional to film thickness. During these AFM and SEM experiments, a very interesting phenomenon was observed. The thin deposited films appeared to be very bright, but the thick films even with the same deposition condition were not bright. This

phenomenon is similar to other reports [11] in literature. The surface roughness could result in the generation of an error in the Dektak thickness measurement, and result in higher resistivity and lower density.

3.2.4 Structure

3.2.4.1 Density

The density measurement of the deposited copper film was carried out by calculating the slope from a plot of film thickness as a function of mass, for deposits on silicon wafer of known area:

$$\text{Density} = \frac{FilmMass(g)}{FilmThickness(cm) \times WaferArea(cm^2)}$$

$$= \frac{10^5}{WaferArea(cm^2) \times Slope \dfrac{cm^2}{g}},$$

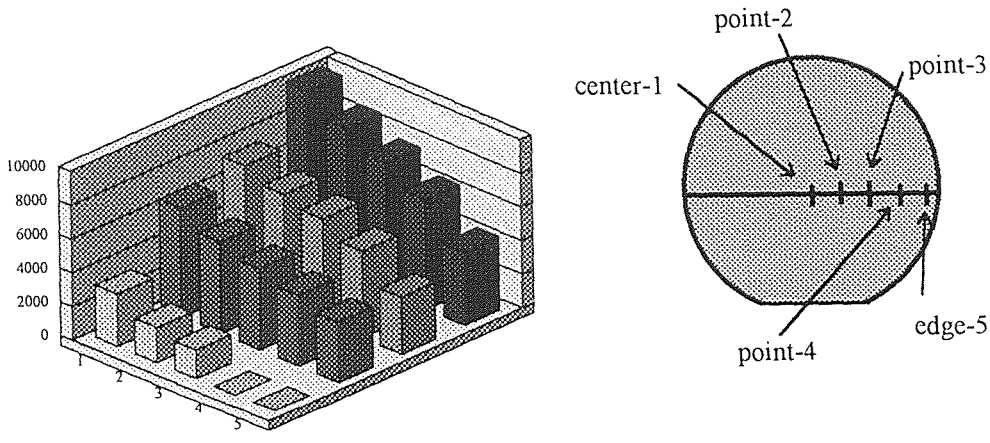

Figure 3.17 The Deviation of thickness profile for four wafers at five points .

from the known wafer area (78.54 cm^2), a density value of 7.40 g/cm^3 was obtained using an average thickness ($AVG_{thickness}=AVG_{(max+min)}$). This value is comparable to the bulk density value (at 20 °C) 8.89 g/cm^3 of copper [32]. The main reasons for the difference between these two values was the deviation of the film thicks across the wafer as shown in Figure 3.19 which resulted from the injection of the precursor near the center of the wafer and surface roughness.

3.2.4.2 Crystal Orientation

The fact that the deposited copper films were polycrystalline was establisshed by XRD (X-Ray Diffraction) as shown in Figure 2.11. It has been suggested that film orientation affects the electromigration and oxidation resistance of metal films [7]. An empirical correlation between increased electromigration lifetime and an increased in the ratio I<111>/I<200>, where I<111> and I<200> are the intensities of reflection from the <111> and <200> crystallographic planes, has been reported by Vaidya et al [11]. Since higher oxidation and electromigration resistance of copper films were expected with a higher ratios, the behavior of <111>/ <200> ratio was studied for the different deposition condition. These results are based on standard reaction condition. In the flow rate study series as shown in Fig 3.20, the value of intensity ratio I<111>/I<200> kept within a certain range 0.55-0.7 for flow rates higher than 6.04 sccm, but when the flow rate was lower than 6.04 sccm, the value of intensity ratio <111>/I<200> increased rapidly with low precursor flow rate. In the pressure study series, shown in Figure 3.21, the value of intensity ratio I<111>/I<200> at a depostion pressure of 50 mTorr point (the lowest

pressure) is higher than the others. However, in temperature study series, shown in Figure 3.20, the value of intensity ratio I<111>/I<200> increased continuously from 200 °C to 140 °C, while at temperatures above 200 °C the value for this ratio within in a limited range. As a result of this trend, the high intensity ratio I<111>/I<200> can be obtained in low growth temperatures, low flow rates and low total pressures, therefore, the intensity ratio <111>/<200> appears to be a strong function of growth parameters as shown in Fig 3.21. Slower growth rates lead to chemical vapor deposition reactions under conditions near equilibrium, and it is believed that slow growth rates could be the reason why higher values of intensity ratio I<111>/I<200> are obtained.

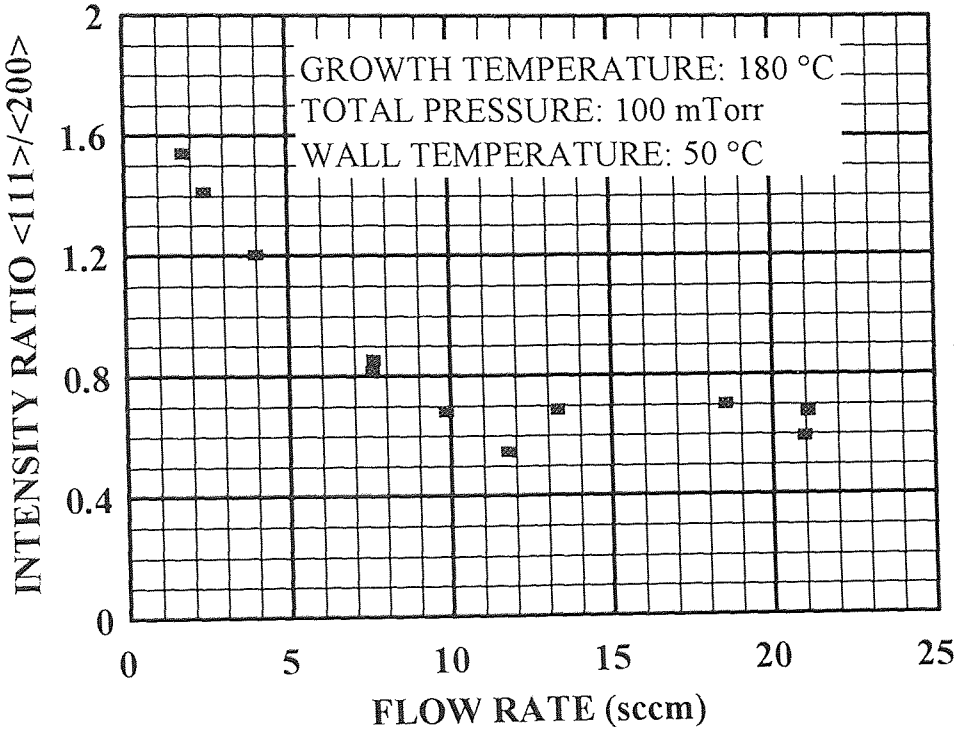

Figure 3.18 Intensity ratio <111>/<200> as a function of precursor flow rate.

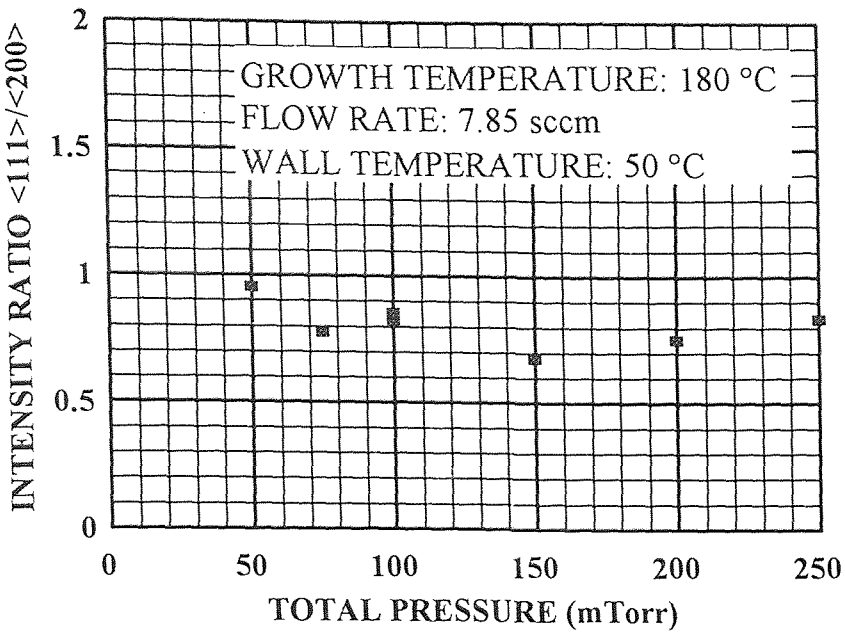

Figure 3.19 Intensity ratio <111>/<200> as a function of precursor flow rate.

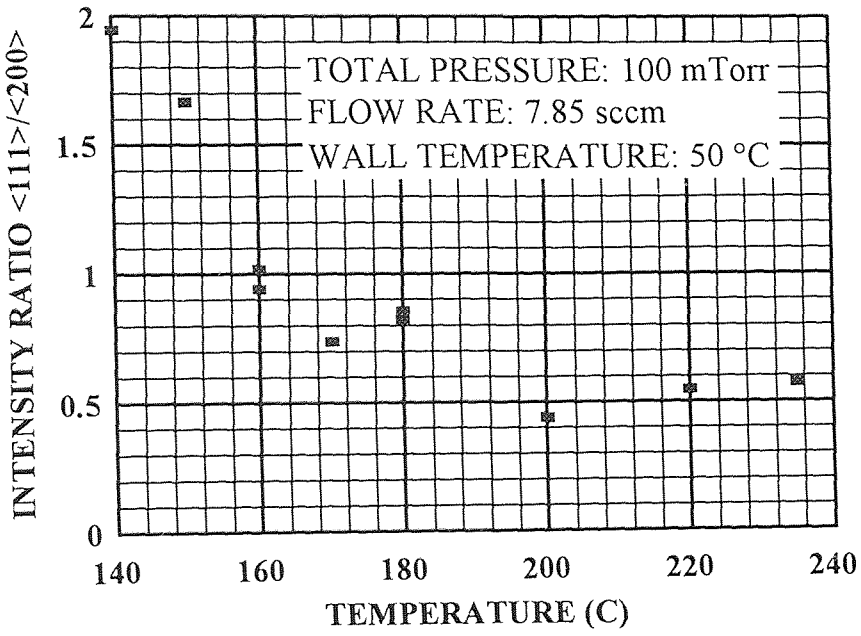

Figure 3.20 Intensity ratio <111>/<200> as a function of growth temperature.

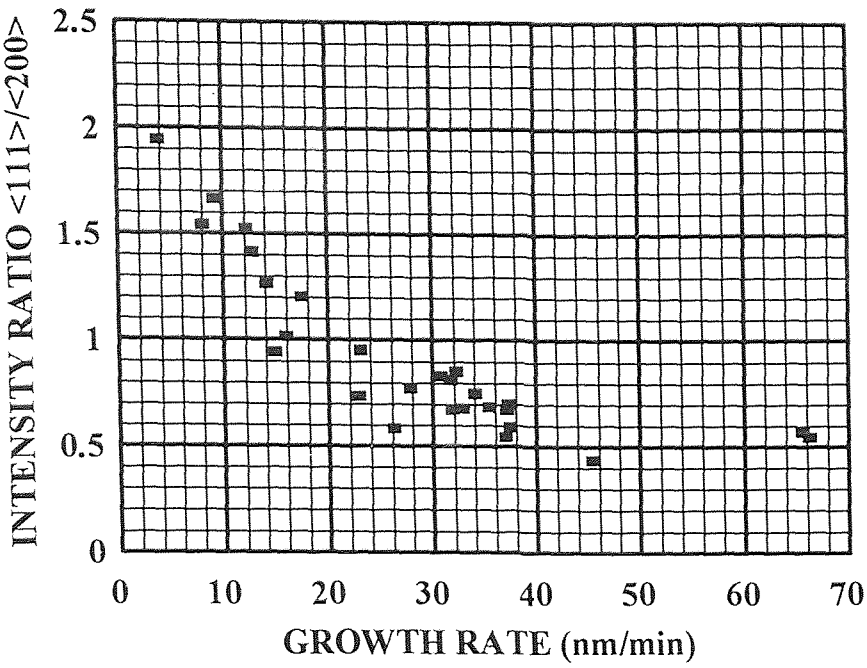

Figure 3.21 Intensity ratio <111>/<200> as a function of growth rate of deposited CVD copper film.

CHAPTER 4

CONCLUSIONS AND SUGGESTIONS

This research included the fabrication and characterization of relatively new CVD Cu film by the precursor Cu(I)(hfac)(tmvs).

High purity copper film had successfully been synthesized on pure silicon wafers in a warm wall, single wafer reactor by low pressure chemical vapor deposition from Cu(I)(hfac)(tmvs) precursor system in the temperature range of 140-250 °C, pressure range of 50-250 mTorr, precursor flow rate range of 4-21 sccm. The feasibility of using Cu(I)(hfac)(tmvs) in LPCVD copper films had been demonstrated through the kinetics studies and film characterization studies. The temperature dependent behavior of deposition rate was found to follow an Arrhenius behavior in the temperature range from 150 to 180 °C with an activation energy of 16.1 kcal/mole. The pressure dependent behavior of deposition rate was found to follow a bimolecular surface reaction model. Low resistivity values (less than 2.2 $\mu\Omega \cdot$ cm) were obtained for as-deposited condition. The X-ray diffraction patterns indicate the polycrystalline nature of as-deposited copper film. AES and XPS spectra reveals the high purity of over 99 percent copper. The surface morphology of the film was observed to roughen with increased film thickness as determined by AFM photos. The crystal orientation varied with growth rate. Furthermore, through the film growth kinetics and film characterization studies, an

optimum film synthesis condition was found a temperatures below 180 °C, total pressure 100 mTorr and precursor flow rate 4 sccm.

The deposition rate of CVD Cu with liquid precursor injection is slightly lower than that of other reports [1], and the resistivity of the CVD Cu is slightly greater than the bulk resistivity. Thickness uniformity and surface smoothness also could be improved. The following suggestions are possible areas of future research to improve the synthesis of CVD Cu films.

(1) Precursor development:

Higher vapor pressure precursor with thermally stable by-products is desirable to achieve higher deposition rate and lower resistivity. Safety also must be considered.

(2) CVD reactor improvement:

For the precursor injection system and liquid controller would improve the controllability and reproducibility of the deposition.

(3) CVD process conditions:

The addition of nitrogen purge gas to the reactor can improve the uniformity of the film.

REFERENCES

1. A. Jain, K.-M. Chi, T. T. Kodas, and M. J. Hampden-Smith, "Chemical Vapor Deposition of Copper from Hexafluoroacetylacetonato Copper(I) Vinyltrimethylsilane" *J. Electrochem. Soc.* 140, 1134 (1993).

2. Jian Li, Tom E. Seidel, and Jim W. Mayer, "Copper-Based Metallization in ULSI Structures" *MRS Bulletin.* XIX, 11 (1994).

3. Ajay Jain, Kai-Ming Chi, Hyun-Koock Shin, Janos Farkas, Toivo T. Kodas, Mark J. Hampden-Smith, "Recent Advances in Copper CVD" *Semiconductor International.* 128 (1993).

4. Pascal Doppelt and Thomas H. Baum, "Chemical Vapor Deposition of Copper for IC Metallization: Precursor Chemistry and Molecular Structure" *MRS Bulletin.* XIX, 42 (1994).

5. A.V. Gelatos, A. Jain, R. Marsh, and C. J. Mogab, "Chemical Vapor Deposition of Copper for Advanced On-Chip Interconnects" *MRS Bulletin.* XIX, 49 (1994).

6. Thomas H. Baum and Carl E. Larson, "Chemical Vapor Deposition from Alkyne Stabilized Copper (I) Hexafluoroacetylacetonato Complexes" *J. Electrochem. Soc.* 140, 156 (1993).

7 Do-Heyoung Kim, Robert H. Wentorf, and William N. Gill, "Film Growth Kinetics of Chemical Vapor Deposition of Copper from $Cu(HFA)_2$" *J. Electrochem. Soc.* 140, 3267 (1993).

8. Ben G. Streetman. *Solid State Electronic Devices*, Third Edition. Prentice Hall, New Jersey, U.S.A., (1990).

9. F. M. d'Heurle, "The Effect of Copper Additions on Electromigration in Aluminum Thin Films" *Metallurgical Trans.* 2, 683 (1971).

10. D. B. Fraser, *Metallization VLSI Technology*, First Edition. S. M. Sze, eds., McGraw-Hill, (1983).

11. Do-Heyoung Kim, Robert H. Wentorf, and William N. Gill, "Low Pressure Chemically Vapor Deposited Copper Films for Advanced Device Metallization" *J. Electrochem. Soc.* 140, 3273 (1993).

REFERENCES
(Continued)

12. Alain E. Kaloyeros and Michael A. Fury, "Chemical Vapor Deposition of Copper for Multilevel Metallization" *MRS Bulletin.* XIX, 22 (1993).

13. S. C. P. Lim, "Reduction of Hillock Formation in Aluminum Thin Films" *Semiconductor Intl.*, pp. 135-144, (1982).

14. J. M. E. Harper, E. G. Colgan, C-K. Hu, J. P. Hummel, L. P. Buchwalter and C. E. Uzoh, "Materials Issues in Copper Interconnections" *MRS Bulletin.* XIX, 23 (1993).

15. Shi-Qing Wang, "Barriers Against Copper Diffusion into Silicon and Drift Through Silicon Dioxide" *MRS Bulletin.* XIX, 30 (1993).

16. N. Misawa, T. Ohba, and H. Yagi, "Planarized Copper Multilevel Interconnections for ULSI Applications" *MRS Bulletin.* XIX, 63 (1993).

17. Michael L. Hitchman and Klavs F. Jensen. *Chemical Vapor Deposition Principles and Applications.* Academic Press, New York, (1993).

18. Hugh O. Pierson. *Handbook of Chemical Vapor Deposition (CVD).* Noyes Publications, New Jersey, U.S.A., (1992).

19. Werner Kern. *Microelectronic Materials and Processes.* Academic Press, New York, (1978).

20. Rosler, R. S. "Low Pressure CVD Production Processes for Poly, Nitride, and Oxide" *Solid State Technol.* 63 (1977).

21. Kern, W., V. Ban, J. L. Vossen, and W. Kern. *Chemical Vapor Deposition of Inorganic Thin Films.* Academic Press, New York, U.S.A., (1978).

22. Kern, W. and R. A. Levy. *Microelectronic Materials and Processes.* Kluwer Academic Press, New Jersey, U.S.A., (1986).

23. Tanikawa, E., T. Okabe, and K. Maeda, "Doped Oxide Films by Chemical Vapor Deposition" *The Electrochemical Soc.* 261, 1521 (1973).

REFERENCES
(Continued)

24. Stering, H. F., and R. C. G. Swann. "Chemical Vapor Deposition Promoted by r.f. Discharge" *Solid State Electronics.* 8 (1965).

25. Claassen, W. A. P., J. Bloem, W. Q. J. N. Valkenburg and C. H. J. Van den brekel. "The Deposition of Silicon from silane in a Low-Pressure Hot-wall System" *J. Crystal Growth.* 57, 259 (1982).

26. Laidler, K. J. *Chemical Kinetics.* Harper & Row. Academic Press, New York, U.S.A., (1987).

27. Cecilia Y. Mak, "Electroless Copper Deposition on Metals and Metal Silicides" *MRS Bulletin.* XIX, 55 (1993).

28. B. Lecohier, B. Calpini, J.-M. Philippoz, and H. van den Bergh, "Copper Film Growth by Chemical Vapor Deposition" *J. Electrochem. Soc.* 140, 789 (1993).

29. "Materials Characterization" ASM Handbook, vol. 10. American Society for Metals, (1992).

30. J. Randall Creighton and John E. Parmiter. "Metal CVD for Microelectronic Applications" *Critical Reviews in Solid State and Materials Sciences.* 18, 175 (1993).

31. Y. Arita, N. Awaya, K. Ohno, and M. Sato. "Copper Metallization Technology for Deep Submicron ULSIs" *MRS Bulletin.* XIX, 68 (1993).

32. William F. Smith. *Principles of Materials Science and Engineering*, Second Edition. McGraw-Hill, New York, (1990).